NAVAL POSTGRADUATE SCHOOL
MONTEREY, CALIFORNIA

THESIS

THE GENERATION AND CHARACTERIZATION OF SURF ZONE AEROSOLS AND THEIR IMPACT ON NAVAL ELECTRO-OPTICAL SYSTEMS

by

Robert Eugene Kiser

March, 1997

Thesis Co-Advisors: Kenneth L. Davidson
C. Russell Philbrick
Roland W. Garwood

Approved for public release; distribution is unlimited.

DUDLEY KNOX LIBRARY
NAVAL POSTGRADUATE SCHOOL
MONTEREY CA 93943-5101

REPORT DOCUMENTATION PAGE

Form Approved OMB No. 0704-0188

1. AGENCY USE ONLY *(Leave blank)*	2. REPORT DATE	3. REPORT TYPE AND DATES COVERED
	March, 1997	Master's Thesis

4. TITLE AND SUBTITLE
THE GENERATION AND CHARACTERIZATION OF SURF ZONE AEROSOLS AND THEIR IMPACT ON NAVAL ELECTRO-OPTICAL SYSTEMS

5. FUNDING NUMBERS

6. AUTHOR(S) Robert Eugene Kiser

7. PERFORMING ORGANIZATION NAME(S) AND ADDRESS(ES)
Naval Postgraduate School
Monterey CA 93943-5000

8. PERFORMING ORGANIZATION REPORT NUMBER

9. SPONSORING/MONITORING AGENCY NAME(S) AND ADDRESS(ES)

10. SPONSORING/MONITORING AGENCY REPORT NUMBER

11. SUPPLEMENTARY NOTES The views expressed in this thesis are those of the author and do not reflect the official policy or position of the Department of Defense or the U.S. Government.

12a. DISTRIBUTION/AVAILABILITY STATEMENT
Approved for public release; distribution is unlimited.

12b. DISTRIBUTION CODE

13. ABSTRACT *(maximum 200 words)*

Aerosols are generated within the surf zone by the breaking of waves along the beachfront. The concentration of aerosols, size and structure of these plumes are impacted by the air/sea temperature differences, breaker type and local winds. During the EOPACE I surf experiment at LaJolla, CA, it was observed that under light wind conditions, standing aerosol plumes would develop to heights of 31 meters. Concurrently, transmittance at FLIR wavelengths would be degraded up to 35%. Similar aerosol plume structures were observed during EOPACE II at Moss Landing, CA. These results are used to characterize and forecast standing plume conditions that may impact Electro-Optical transmission..

14. SUBJECT TERMS Environmental Data, Electro-Optical, Surf Aerosols, EOPACE, Aerosol Plumes	15. NUMBER OF PAGES 75
	16. PRICE CODE

17. SECURITY CLASSIFICATION OF REPORT	18. SECURITY CLASSIFICATION OF THIS PAGE	19. SECURITY CLASSIFICATION OF ABSTRACT	20. LIMITATION OF ABSTRACT
Unclassified	Unclassified	Unclassified	UL

NSN 7540-01-280-5500

Standard Form 298 (Rev. 2-89)
Prescribed by ANSI Std. 239-18 298-102

Approved for public release; distribution is unlimited.

THE GENERATION AND CHARACTERIZATION OF SURF ZONE AEROSOLS AND THEIR IMPACT ON NAVAL ELECTRO-OPTICAL SYSTEMS

Robert Eugene Kiser
Lieutenant Commander, United States Navy
B.S., United States Naval Academy, 1982

Submitted in partial fulfillment
of the requirements for the degree of

MASTER OF SCIENCE IN METEOROLOGY AND PHYSICAL OCEANOGRAPHY
from the
NAVAL POSTGRADUATE SCHOOL
March 1997

DUDLEY KNOX LIBRARY
NAVAL POSTGRADUATE SCHOOL
MONTEREY CA 93943-5101

ABSTRACT

Aerosols are generated within the surf zone by the breaking of waves along the beachfront. The concentration of aerosols, size and structure of these plumes are impacted by the air/sea temperature differences, breaker type and local winds. During the EOPACE I surf experiment at Scripps Pier LaJolla, CA, it was observed that under light wind conditions, standing aerosol plumes would develop to heights of 31 meters. Concurrently, transmittance at FLIR wavelengths would be degraded up to 35%. Similar aerosol plume structures were observed during EOPACE II at Moss Landing, CA. These results are used to characterize and forecast standing plume conditions that may impact Electro-Optical transmission.

TABLE OF CONTENTS

I. INTRODUCTION

With the Navy's renewed interest in the coastal environment, effort is being focused to study the impact of surf zone generated aerosols. In the past, many studies have observed and modeled the generation of open ocean aerosols from whitecaps, but very little work has been done in the surf zone area. More important than the generation process, the need was identified to access the effect on electro-optical (EO) transmission across this zone to determine the impact on military operations. This coastal mesoscale phenomenon was assigned to several groups for study, with overall coordination by the Naval Command Control and Ocean Surveillance Center, Research and Development (NRaD) (Jensen, 1995).

A. BACKGROUND

Navy operations are carried out in geographic locations ranging from "open ocean" to "coastal environmental" conditions under the threat of air-, surface-, and land-launched anti-ship cruise missiles which are difficult to detect and track in a cluttered environment. Fleet units operating in the open ocean, or in coastal regions, must be able to detect and/or track such sophisticated weaponry. The Navy is presently developing and/or utilizing infrared technology for the detection or identification of such physical threats. Infrared Search and Track systems (IRSTs) provide the capability of continually scanning the ocean/coastal horizon for detection of high speed, low flying incoming missiles and fast attack, low profile, high speed patrol boats. Forward Looking IR Radar (FLIR) provide pilots with the capability of target detection/identification as well as night-time images of the terrain over which they are flying. FLIRs are currently used in reconnaissance aircraft and are under

development for submarine periscopes. The degradation of radiance contrast between a target and its natural background, as viewed by an infrared sensor, is determined by the constituents of the intervening atmosphere which absorb, emit and scatter the radiation. At optical wavelengths where scattered radiation is necessary to see a target, visibility threshold has been defined as the case when 2 percent of the scattered radiation from the target reaches the observer. This corresponds to the point when contrast definition is lost. A logical way to describe the IR visibility limit, assuming that machine vision can be comparable to the human eye, is the case when the sum of the scattered and emitted radiation from the target is more than plus or minus 2 percent different from the sum of the radiation scattered, absorbed and emitted along the intervening path. For viewing angles close to the horizon, both the absorption by the trace and well mixed atmospheric gases together with the absorption and scattering by aerosols determine the atmospheric transmittance. Atmospheric aerosol models presently employed, such as LOWTRAN, are inadequate for representing IR propagation in coastal environments. Modeling efforts need to be undertaken which better describe the coastal effects of aerosols, and incorporate them into LOWTRAN to better predict performance of EO systems used for detecting low-altitude targets.

Strike warfare planning and vulnerability assessment rely on tactical decision aids (TDA's). The Electro-Optical Decision Aid (EOTDA), primarily developed by the U.S. Air Force for Air Force applications, is being incorporated into Naval environmental prediction systems such as the Tactical Environmental Support System (TESS), version 3.0, and the Tactical Aircraft Mission Planning System (TAMPS). These systems are the primary tool of the Naval Meteorology and Oceanography (METOC) officer for support in the coastal

region. There is no TDA presently available that can predict EO system performance across the transition zone from open water to land.

B. EOPACE

A program entitled "EO Propagation Assessment in Coastal Environments" (EOPACE) was initiated to measure and analyze the performance of EO weapons and sensor systems operating in the coastal environment. The EOPACE program is an ongoing effort and has been conducted along the central and southern California coast with participants from the United States and NATO countries. The primary objectives of this program are to:

1) Quantify effects of coastal aerosols on EO propagation extinction

2) Develop mesoscale models and data assimilation systems

3) Evaluate EO system performance across the surf zone

The effort to quantify effects caused by aerosol extinction include: 1) a definition of an air-mass parameter for coastal regions, 2) measurement and modeling of small aerosols and their chemistry, 3) measurement of surf-generated aerosols, 4) sensing of aerosol extinction with lidar, satellite-based techniques and other advanced sensor, and 5) near-surface transmission measurements.

The evaluation of EO systems performance included the adaption of the Air Force developed Electro Optical Tactical Decision Aid (EOTDA) for Navy use; development of background, target, and clutter (including land) models; use of polarization to improve target discrimination; and evaluation of IRST and FLIR systems.

One key feature of EOPACE is to conduct general observation programs over a three year period with intensive use of unique observational techniques. The observations assure

encountering the full range of atmospheric conditions. Special emphasis is to be given to aerosols generated in the surf zone and long term background/clutter measurements. During the intensive observation periods various thermal images and IRSTs will be deployed. The Office of Naval Research (ONR) funded most of the EOPACE investigation and EO sensors such as IRSTs and FLIRs.

C. COASTAL AEROSOLS

Aerosol in the coastal marine environment are becoming an increasingly important concern for the modern Navy. Diverse underlying threats range from speeding patrol boats in shallow waters to missiles approaching from over the horizon. Infrared (IR) and EO systems are an important complement to existing radar systems for the surveillance, detection and identification of these threats but they are sensitive to the coastal aerosols. Coastal areas have been overlooked in the past in preference to the less complex open ocean situations. There are a number of aspects of the coastal aerosols which are not well understood. The purpose of the EOPACE experiment is to investigate these aspects to provide a twofold payoff: 1) the development of an effective coastal aerosol model, CAM, which would estimate the aerosols and their optical effects based on measurable parameters, and 2) the investigation of possible remote sensing techniques for assessing these aerosols.

One source of sea salt aerosol in the coastal regime is the surf-generated aerosol. Storm-generated swell together with normal wind waves hitting the shoreline produce an extensive border of white water in coastal areas. The production of aerosols in this area is not directly wind related and a white water belt is often seen along the coast, even in the presence of a calm sea.

In the coastal white water region, additional aerosol production sources of jet drops, spray, and perhaps other processes, are important in the description of the density and size distribution of aerosols. Characterization of all sources has not been accomplished, but only crude estimates of their importance have been made. Initial estimates from the Coastal Aerosol Workshop indicate that more than 10% of the typical ocean environment aerosols were generated in the surf zone. In certain low wind situations, the only source locally generated aerosols is from the surf. The first recommendation of the workshop (Jensen, 1995) was the need to study specific mechanisms that generate droplets in the surf zone.

The southern California region is an ideal area to study surf-generated aerosol and to quantify the effect of surf aerosol in the overall Marine Boundary Layer (MBL) description. The southern California area is subjected to an extremely long fetch where remote storms in the south Pacific often produce significant swell even during periods of relatively calm winds, and minimal wind waves. This allows an easy separation of surf- and wind -generated sea salt aerosol.

The reason for trying to properly describe the density, type and size of aerosols is that such a description will allow the determination of the optical extinction characteristics at any wavelength in the optical spectrum. Although, aerosol spectra were not obtained by laser illumination in this study.

II. LASER SCATTERING FROM SURF AEROSOL

To visualize the generation, density and movement of surf zone aerosols, a laser scattering instrument was developed and operated by the Applied Research Laboratory (ARL) Remote Sensing/Electrical Engineering Department of the Pennsylvania State University. It was used in similar configuration for both Phases I and II of EOPACE. Phase I was conducted at Scripps Pier San Diego from 22 January to 9 February 1996, and Phase II was conducted at the Marine Laboratory Pier at Moss Landing (Monterey Bay) from 4 to 16 March 1996. The primary goal of the laser measurements was to characterize the surf aerosol plume structure. This was accomplished using a vertically fanned laser beam transmitted over the ocean's surface and imaged by two thermoelectrically cooled high resolution Charge Coupled Device (CCD) cameras. The main concept of this experiment was to illuminate a laser sheet perpendicular to the beach, fanning vertically out to sea and using these specialized cameras offset at angles of 10° to 50° from the laser sheet to image the brilliant Mie back scatter of the laser from newly generated surf aerosols. Figure 2.1 illustrates the reflection pattern for Mie scattering showing the concentrated forward scatter and the secondary back scattering peaks at approximately 150 and 180 degrees.

The experiment layout and precise location of the laser and cameras (positions A,B,C & F) differed very slightly between the Scripps Pier (Figure 2.2) and Moss Landing Pier (Figure 2.3). The primary difference between the two locations was that the laser sheet was oriented at an angle to the Scripps Pier, while it was parallel to the Moss Landing Pier. This slight difference in configuration only impacted the geometrical processing of the data to

obtain the height of plume versus distance along the pier profiles.

The transmitter used to produce the vertical laser sheet was an argon-ion (green) laser operating at 514.5 nm. The laser beam was then passed through a negative cylindrical lense to fan it out vertically and then reflected off a mirror at a 45 degree angle over the surf zone as depicted in Figure 2.4. A polarizing waveplate was also used to create horizontal and vertical polarization. Two digital imagers were used with 8.5μm focal length lenses and were placed to measure back scattered signals at angles of approximately 170 and 150 degrees from the incident beam.

Data sets were taken in a series of 10 images, with the orientation of the electric field alternating between vertical and horizontal polarization modes. Each synchronized image set was separated by approximately 25 seconds while the image was downloaded by the computer and the camera was reset. Figure 2.5 illustrates the camera positioning during the Moss Landing experiment. In addition, a video camera and still camera were placed at the laser site (back scatter) or at the end of the pier (forward scatter) for portions of the measurement period. Figures 2.6 and 2.7 are examples of still photographs taken during light surf conditions at Moss Landing. Environmental conditions such as air temperature, humidity, wind and wave information were recorded in addition to the laser scattering data. All images are 512 x 768 pixels with a resolution of 16 bits/pixel.

A. EOPACE PHASE I, SCRIPPS PIER SAN DIEGO

During EOPACE Phase I in San Diego, in addition to the laser illumination of the plumes, transmittance was measured across the surf zone using an infrared spectrometer to measure the signal from a source collimator. The configuration and specification of the

transmission equipment was similar to that described by Carlson, et al (1995). The collimator was collocated with the laser, while the spectroradiometer was positioned at the end of the pier in the vicinity of the zero angle reference point illustrated in Figure 2.2. The atmospheric transmission is calculated using measurements of the IR signals received over a short and long path of transmission using the definition of transmittance (T).

$$T = e^{-\sigma(R2 - R1)}$$

Where: σ = attenuation coefficient
R1 = short path length
R2 = long path length

The source for this transmittance measurement was a 5-inch diameter collimator. This is a clear-aperture with a 38-inch focal length optical system coupled to a Blackbody source. The emissivity of the Blackbody source is 0.99 with an operating temperature of approximately 1000°C (±1.5°). This collimator system incorporates a two-optical element Newtonian telescope system enclosed in a 5-inch diameter cylinder mounted on a 1 meter tripod.

The infrared spectrometer used to measure the source signal covers the wavelength spectra from 1.0 to 14.9μm, similar to the upper and lower frequencies used by FLIR. The average spectral resolution is 0.018μm in the 3-5μm region and 0.06μm in the 8-14μm region. A complete spectral scan is accomplished in approximately 13 seconds.

Transmittance measurements were made at various times throughout the daytime and evening hours, while illumination of the surf-generated plumes by the laser scattering instrument was restricted to evening hours only (the green argon-ion laser back scatter would

not have been detectable above the daytime visible background). The optical path for the transmittance measurement was set at approximately 5 m above the sea surface. A detailed analysis of the transmittance and plume structure data for San Diego will be discussed in Chapter V.

B. PLUME GENERATION

It is necessary to examine the differing aspects of aerosol plume formation and influencing factors within the surf zone and in the open water. The vertical laser sheet over the surf zone helps to visualize the generation, development, movement and disbursion of the surf-generated aerosol plumes. From observation of these plume structures, it is apparent that their formation is linked to several complex variables including breaker type, air-sea temperature difference, relative humidity and wind characteristics.

Much research has been done in the area of maritime aerosol generation by whitecaps in open water as described by Fairall and Davidson, 1986. Fewer studies have been conducted to characterize the generation of the sea aerosols in the surf zone region. A striking differences between open water generation and surf zone generation is the path of the trapped air bubble that generates the jet and film droplets that become aerosols. In the open ocean, as well as in the surf, large quantities of air are introduced into the water with white capping. This air is entrained into the water by the gravitational force of the breaking wave, once in the water it is forced to some depth where upward buoyant forces take over, and finally the bubble bursts as it reaches the ocean surface ejecting liquid aerosols into the atmosphere (Resch, 1986). The stronger the wind, the greater the whitecapping and the greater the quantity of air bubbles generated. Figures 2.8 and 2.9 are simple schematics of

open water aerosol generation.

In the open water the bubbles follow oscillating orbits similar to the water particles within the wave itself. However, in the surf zone region, as the water depth shoals toward the beach it becomes impossible for the oscillating water particles to complete their orbits. At a depth of water roughly equal to 1.3 times the wave height, the wave becomes unstable (Bortkovskii, 1987). This happens when not enough water is available in the shallow water ahead to fill in the crest and complete a symmetrical wave form. The top of the onrushing crest becomes unsupported and it collapses, falling in incomplete orbits. As the crest tumbles forward falling into the trough ahead, the momentum carries the separated water toward the beach face.

The quantities of air bubbles formed are a function of the type of breaker (Bortkovskii, 1987). In plunging breakers, the water in the crest, attempting to complete its orbit, is hurled ahead of its steep forward side and lands in the trough. As the upper part of the wave collapses air is entrapped, resulting air bubbles reach the surface and liquid aerosol droplets are formed in great quantities. Spilling breakers have more of a gradual release of energy, with the crest tumbling down a more gently sloping wave face. The entrapped air (bubble) is released in a more gradual fashion. We can assume plunging waves produce more bubbles than spilling breakers.

Another influence on the development of aerosol plumes is the instability of the internal boundary layer (IBL). The air layer that is modified by flow over a different surface is called an IBL because it forms within an existing boundary layer (Stull, 1988). We will focus on the turbulent mixing due to the warm ocean with the cold atmosphere above (Figure

2.10). Because the surface heat flux from the ocean to the air changes between the land and water surfaces, the region of the modified air is called the thermal internal boundary layer (TIBL). The TIBL will determine the stability of the air mass above the sea surface where these liquid aerosols are being injected and either inhibit or enhance the development of the plumes by thermal convection. In an unstable TIBL injected aerosol would continue to rise above it's maximum height of ascent under neutral conditions. Conversely, in a stable TIBL the ascent of this same particle would be retarded. In the formation of aerosol plumes, the strongest and tallest plumes would be associated with strong plunging breakers when the ambient air temperature is cooler than the sea surface temperature. This condition existed during both phases of EOPACE with the temperature difference ranging between 3-5°C in San Diego and averaging around 1°C at Moss Landing.

Once the aerosol plumes are formed, the local wind can have a dramatic impact on the plume structure and intensity. Wind speed has a direct impact on the maximum development height of these structures. As wind speed increases, the development height decreases because of thermal instability and , hence, vertical motion is decreased. The vertical velocities are dampened by shear induced turbulence, resulting in less vertical development. Additionally, the direction of the wind component also impacts the plume structures. An offshore breeze creates more turbulence from the rougher land surface and normally brings with it drier air. This enhances increased mechanical turbulence which breaks up plumes and it also enhances entrainment mixing causing dilution and drying of the plume structures. An onshore breeze brings less turbulence and moist air into the generation area and can cause enhancement of the plumes.

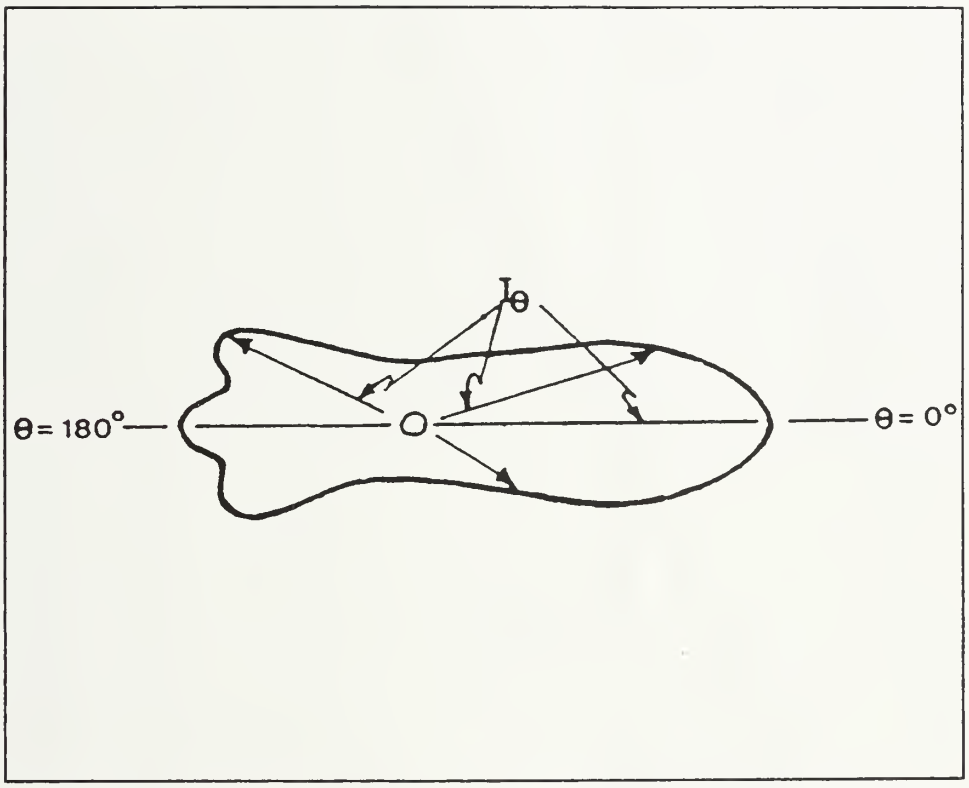

Figure 2.1 Mie back scatter is focused between approximately 130 and 150 degrees. (From Deirmendjian, 1969).

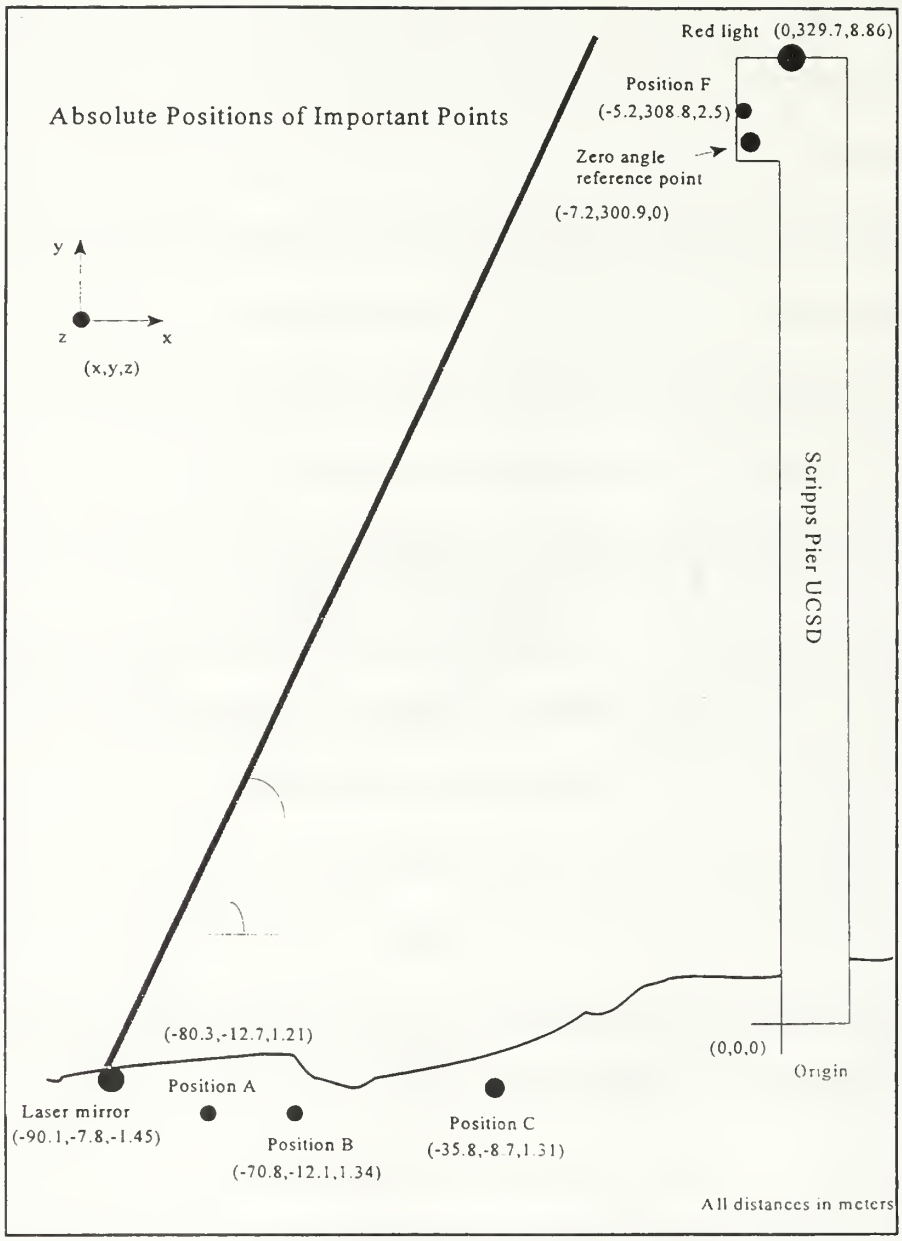

Figure 2.2 Scripps Pier San Diego, laser and camera geometry during EOPACE Phase I. (From Philbrick, et al 1996).

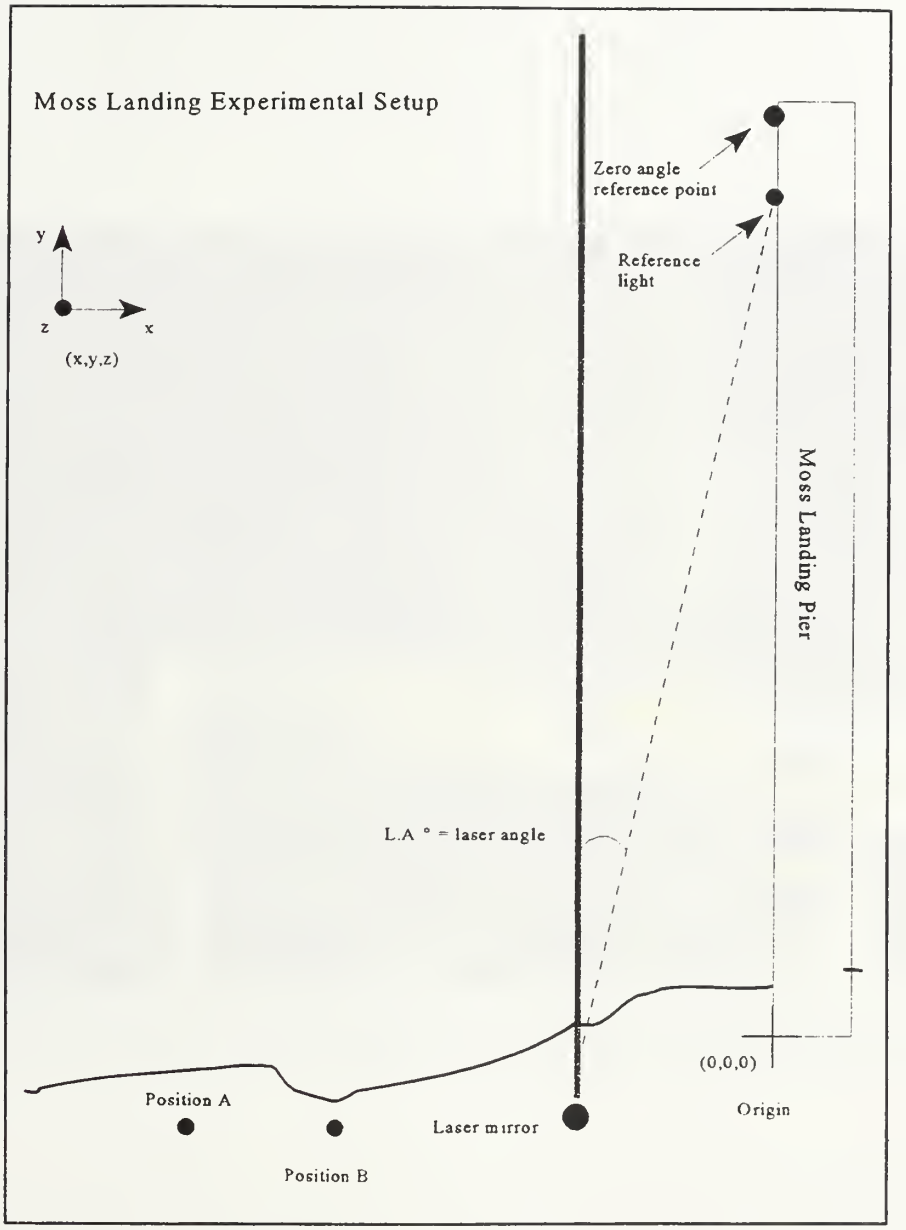

Figure 2.3 Moss Landing Pier laser and camera geometry during EOPACE II. (From Philbrick, et al 1996).

Figure 2.4 Penn State's Laser Scattering 514.5 nm Argon-ion (green) laser configuration from emitter through negative cylindrical lense, polarizer and reflecting mirror.

Figure 2.5 Thermoelectrically cooled high resolution images as positioned during the Moss Landing Phase of EOPACE. In the picture are the author in the foreground and PSU graduate student Bill Durbin in the background, each are operating the digital imaging cameras.

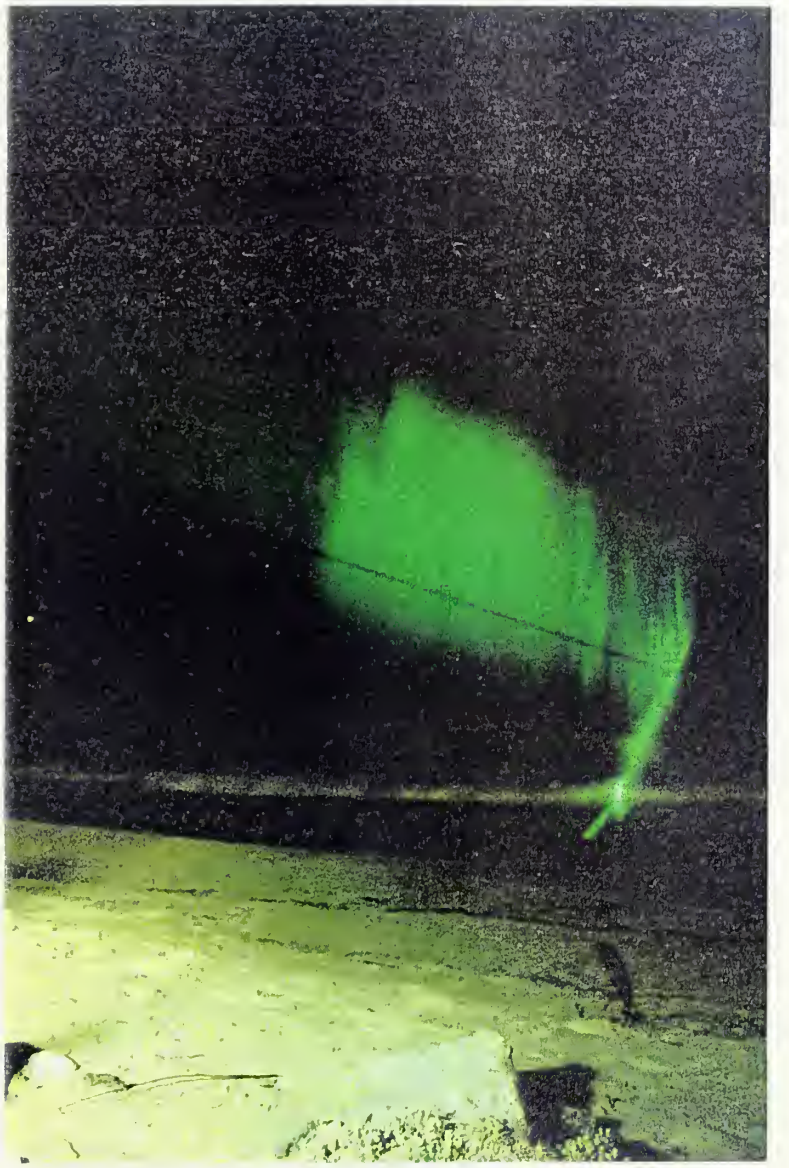

Figure 2.6 The laser fan projected over the surf zone at Moss Landing illuminates the back scatter of aerosols generated within the near shore breaker zone.

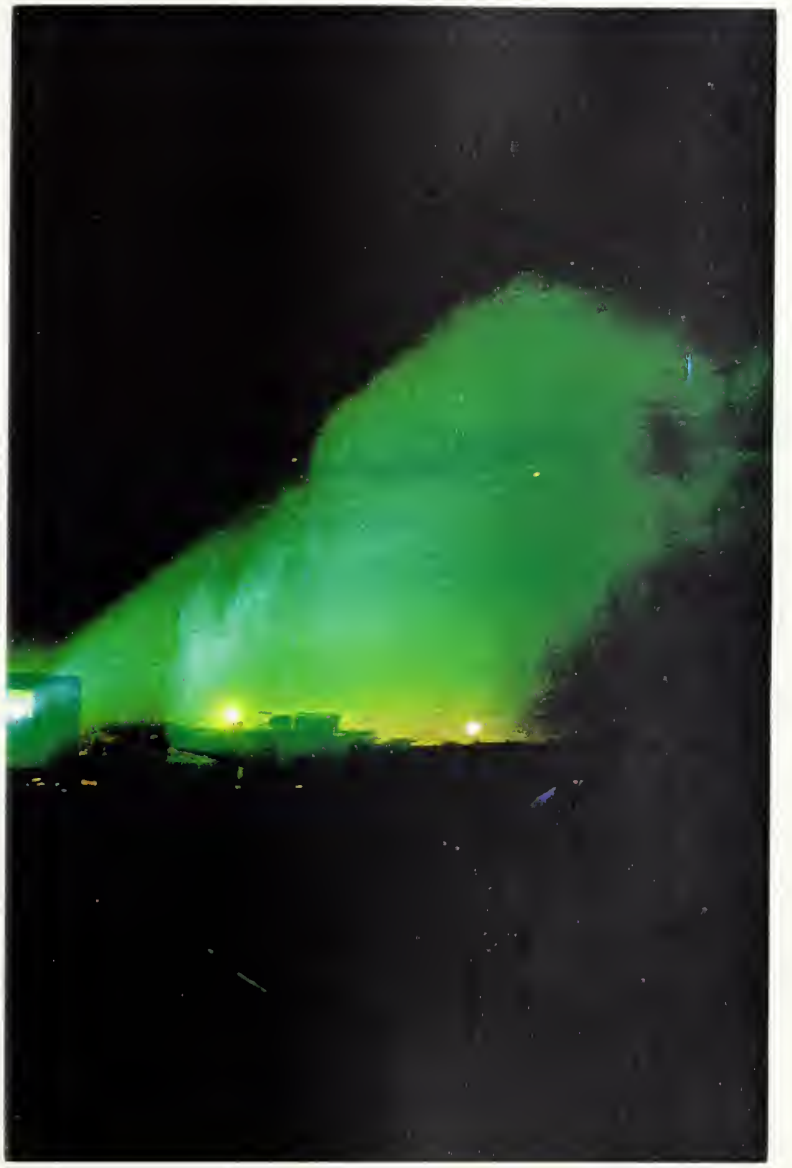

Figure 2.7 With the camera located near the end of the pier at Moss Landing, the laser fan is visible with stronger forward scatter from developing plumes.

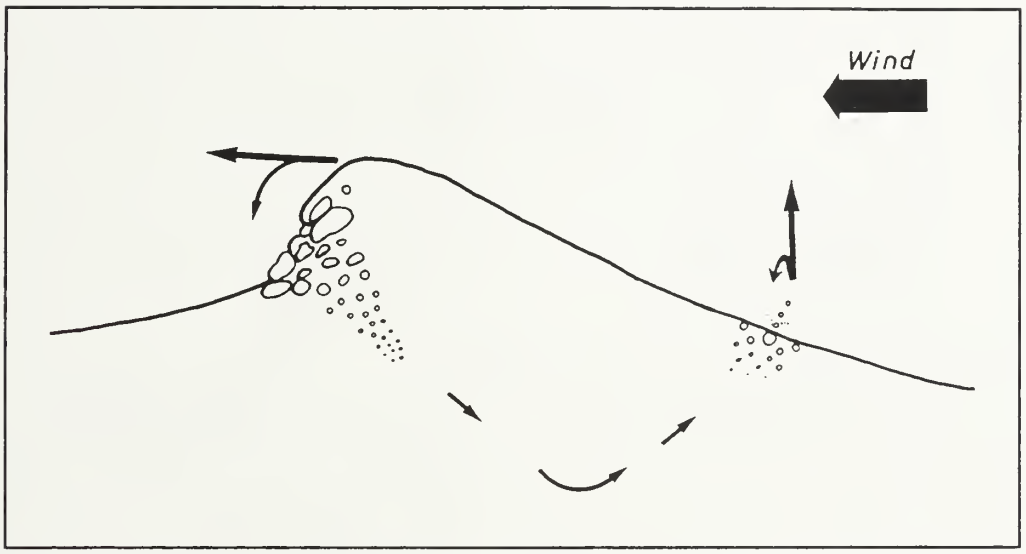

Figure 2.8 Maritime aerosols are normally generated by entrapped air pockets created by breaking waves. These air pockets are mechanically pushed down until the buoyancy of the bubbles ascend toward the surface. As the bubbles burst at the surface, aerosols a created and dispersed by the local winds. (From Resch, 1986).

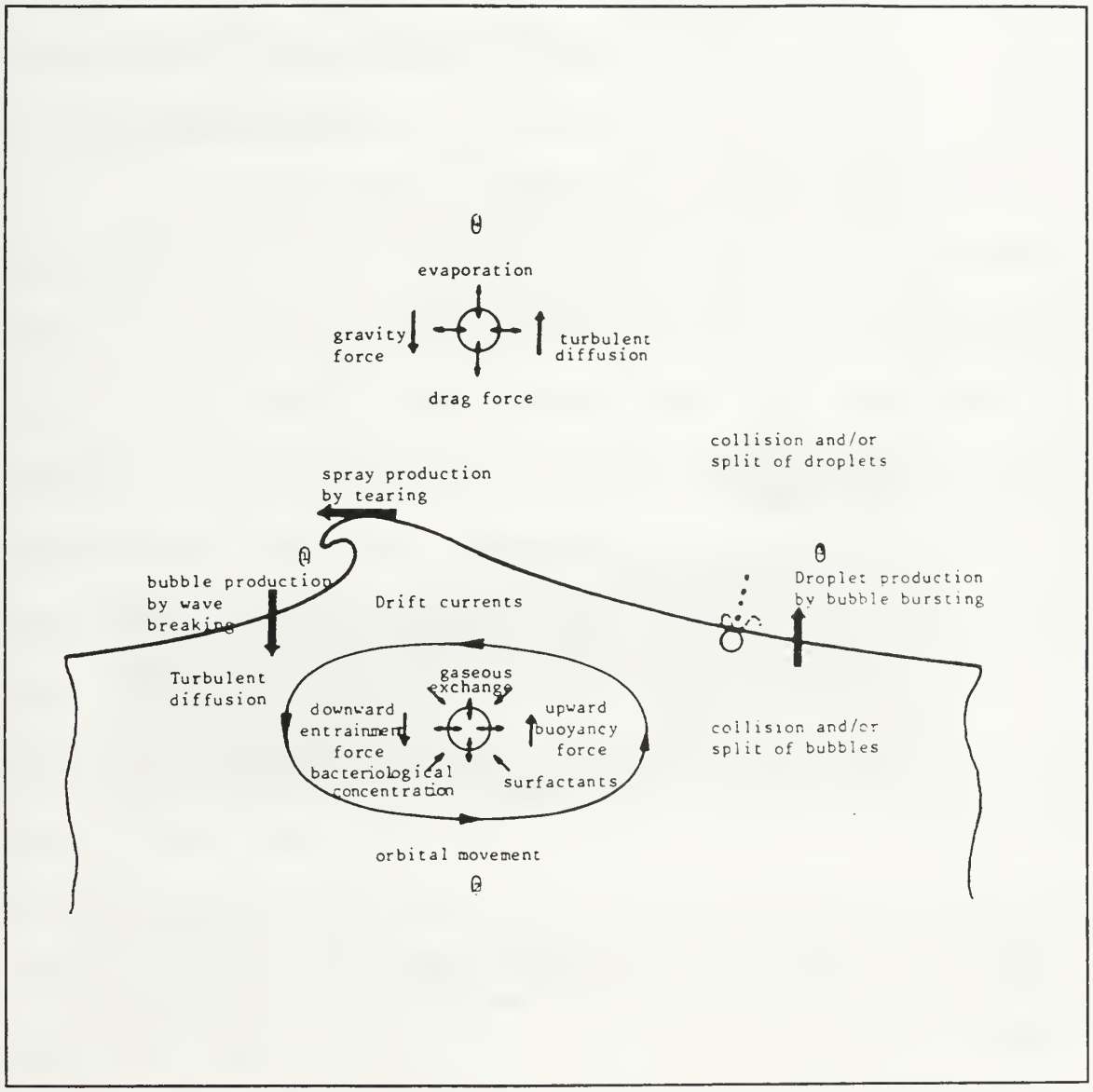

Figure 2.9 Many various and complex forces are involved in the process of air-sea particulate exchange. (From Resch, 1986).

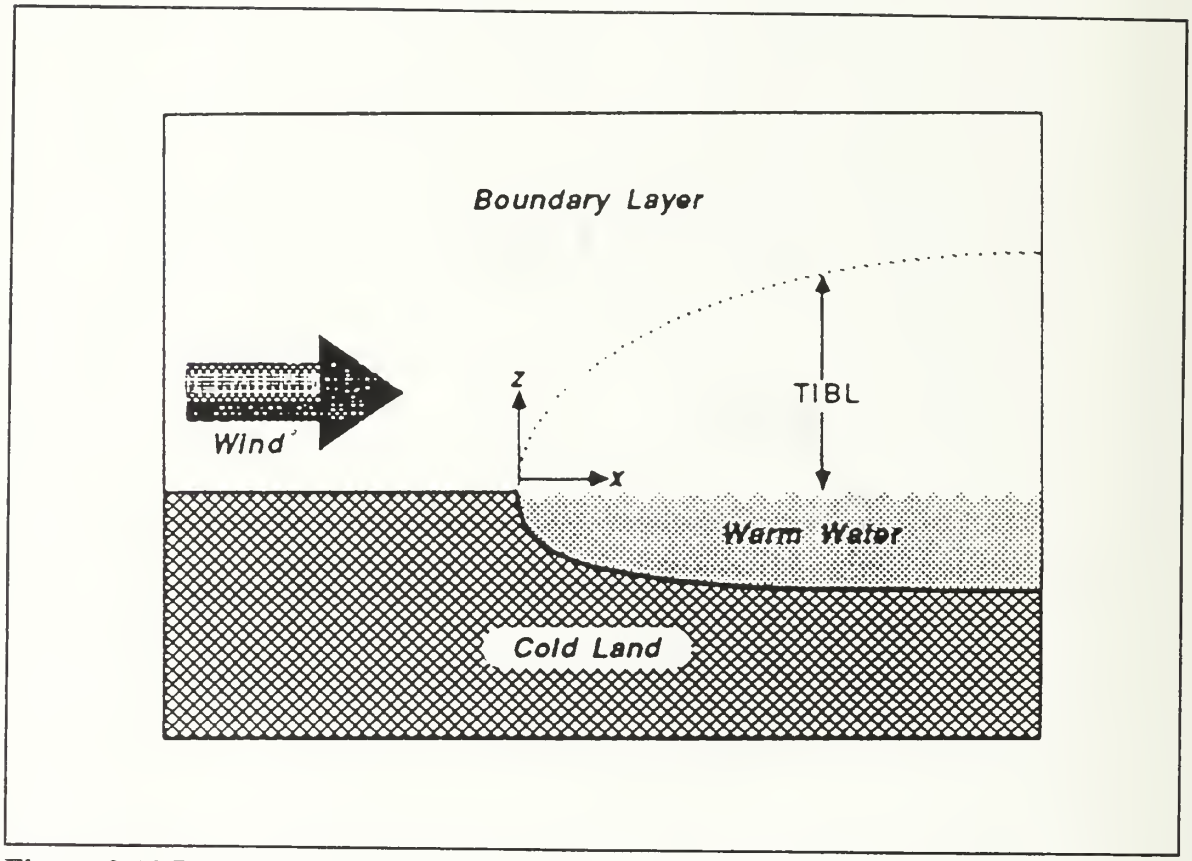

Figure 2.10 Processes involved in the development of a convective thermal internal boundary layer (TIBL) with warm dry air blowing offshore over cooler water. The TIBL represents the unstable heat-flux discontinuity that grows within the boundary layer. (From Stull, 1988).

III. PLUME OBSERVATIONS

Three classifications of aerosol plumes were identified from data obtained with the laser scattering instrument configuration, previously described.

A. ON-SHORE WEDGE

The plume structure, which is associated with on-shore winds of greater than 5 kts, water temperature greater than land temperature and plunging breakers, is the on-shore wedge. As the aerosols are generated, they are advected on-shore and orographically lifted by the beach slope. With flow from a warmer to a cooler surface, a stable TIBL forms analogous to the nocturnal boundary layer. Once overland, the residual turbulence within the plume quickly starts to decay. Static stability suppresses turbulence except near the surface where irregularities and shear cause low level turbulence to occur. Turbulence decreases with height to a poorly defined plume top and dry air entrainment evaporates and disperses the liquid aerosols in the lower portion of the plume. Scattering within the illuminating laser sheet is very weak. Figures 3.1 and 3.2 show the typical on-shore wedge plume structure.

B. STANDING PLUMES

Standing plumes, are associated with wind speeds less than 3 kts, water temperatures greater than overlying air temperature and plunging breakers. These plumes are comprised of many narrow columns of aerosols that have a great density (large scattering signature) and develop to heights above 35 m. As illuminated by the laser, the breaking waves have large puffs of aerosol rising vertically from the surf area. Figures 3.3 and 3.4 are examples of a standing plume.

C. OFFSHORE WEDGE

An offshore wedge forms with wind speeds of greater than 5 kts blowing offshore, water temperature greater than the advected terrestrial air mass, and plunging breakers. As the aerosols are injected into the atmosphere by the breaking waves, they are sheared offshore. Due to the coastal topography and dry air mass, severe turbulent mixing can be noted at the aerosol/air interface. This aerosol wedge is identical to the convective Thermal Internal Boundary Layer (TIBL) described by Stull (1989). As the air flows from a cooler to a warmer surface, a steady state convective mixed layer (convective TIBL, in this case) forms and deepens with distance downwind of the shoreline. Turbulence is vigorous over the bulk of the convective TIBL, and a relatively sharp, well defined top exists. As the aerosol plumes advect downwind, the plume warms, the temperature difference between the air and sea surface lessens. As a result, the plume becomes less buoyant and the ascent rate of the plume is reduced. At a distance downwind of the shoreline, the plume is assumed to reach a steady state of equilibrium with the sea surface, resulting in reduced buoyancy and little or no entrainment. The aerosols lose their buoyant uplift and gravity eventually takes its toll on the aerosols resulting in a lowering and stratification of the mixed layer. Figures 3.5 and 3.6 are examples of the typical off-shore wedges seen at both Scripps and Moss Landing piers.

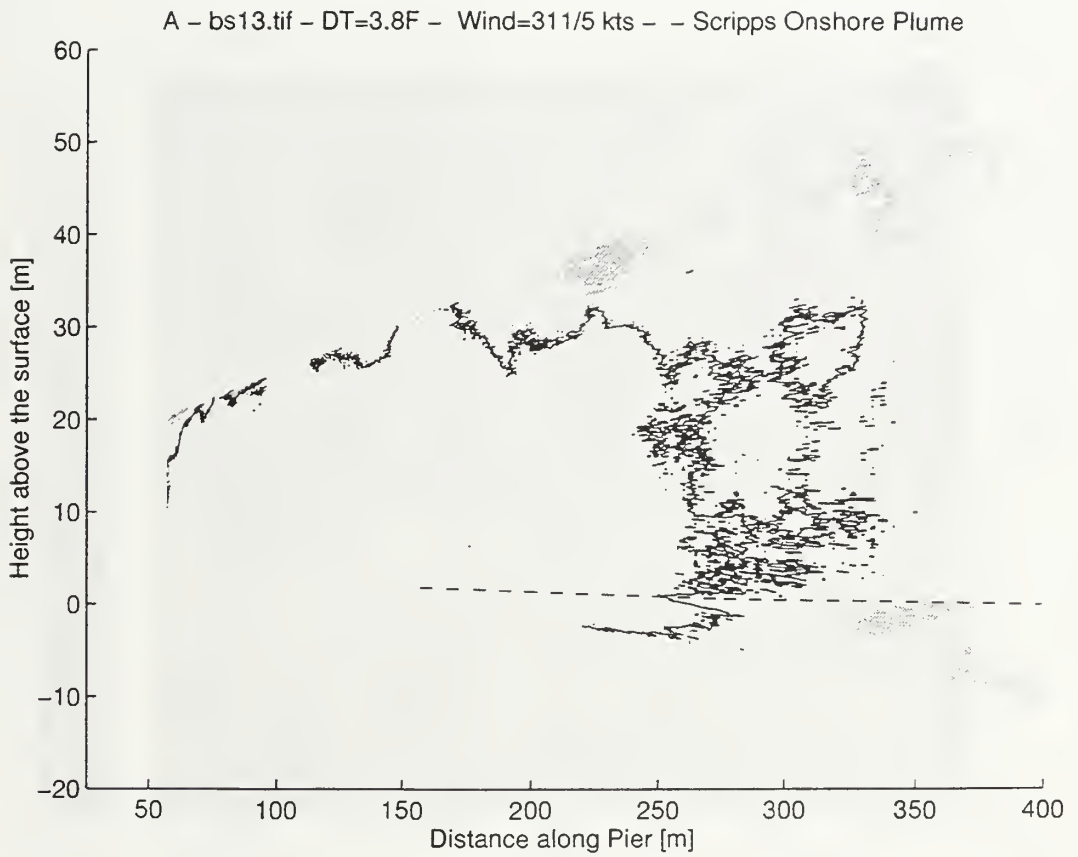

Figure 3.1 Scripps Pier on-shore plume. Uniform plume height of approximately 27-30 m advected onshore by 5 kt wind.

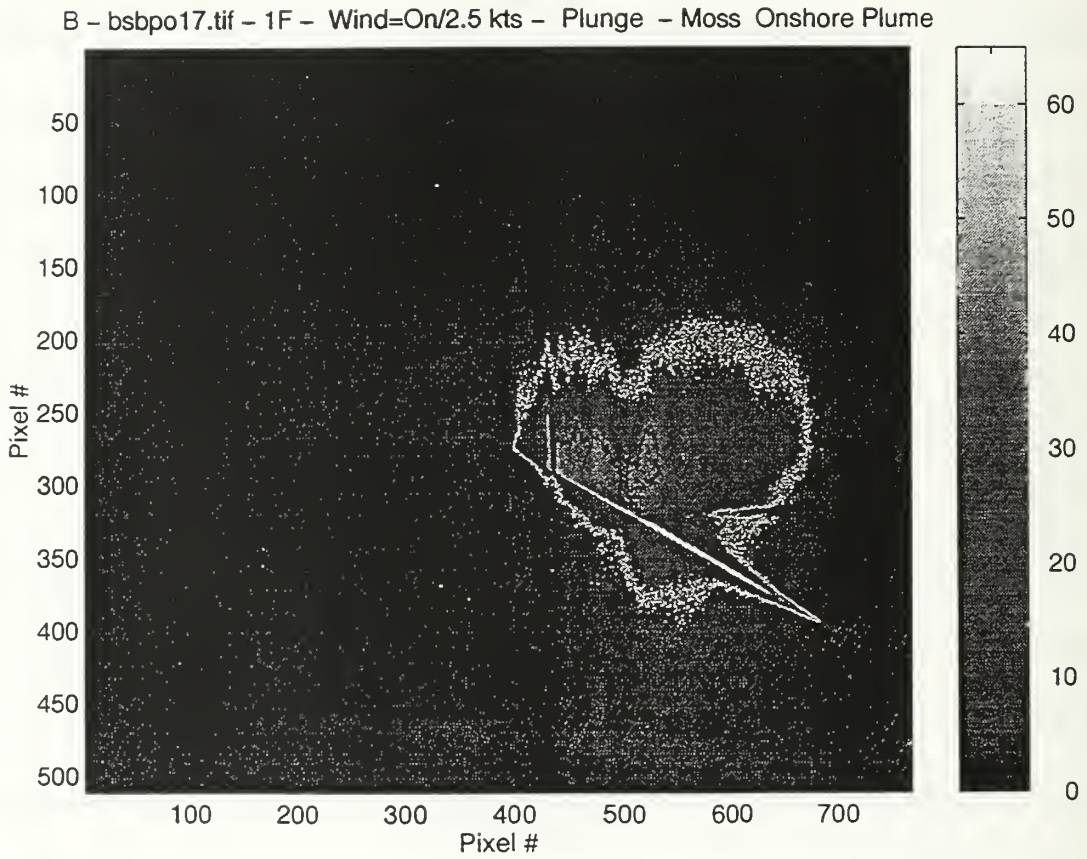

Figure 3.2a Processed pixel image of laser sheet back scatter of Moss Landing onshore plume from the thermoelectric camera. Grade shade scale adjusted to optimize contrast of upper limit of plume. The bright line shows trace of lower edge of the fanned beam on the water surface.

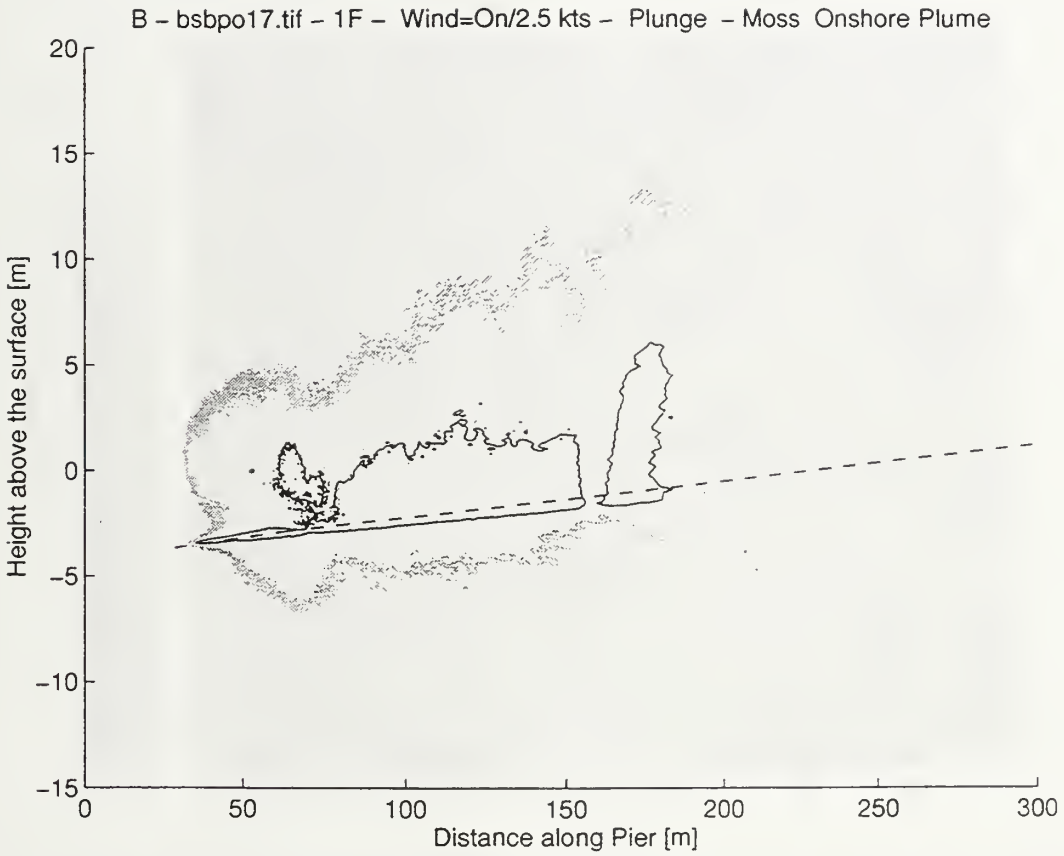

Figure 3.2b Resolved pixel image of figure 3.2a, displaying height of plume along the pier perpendicular to the beach face. Note uniform plume of 8-11 m being advected onshore by 2.5 kt wind

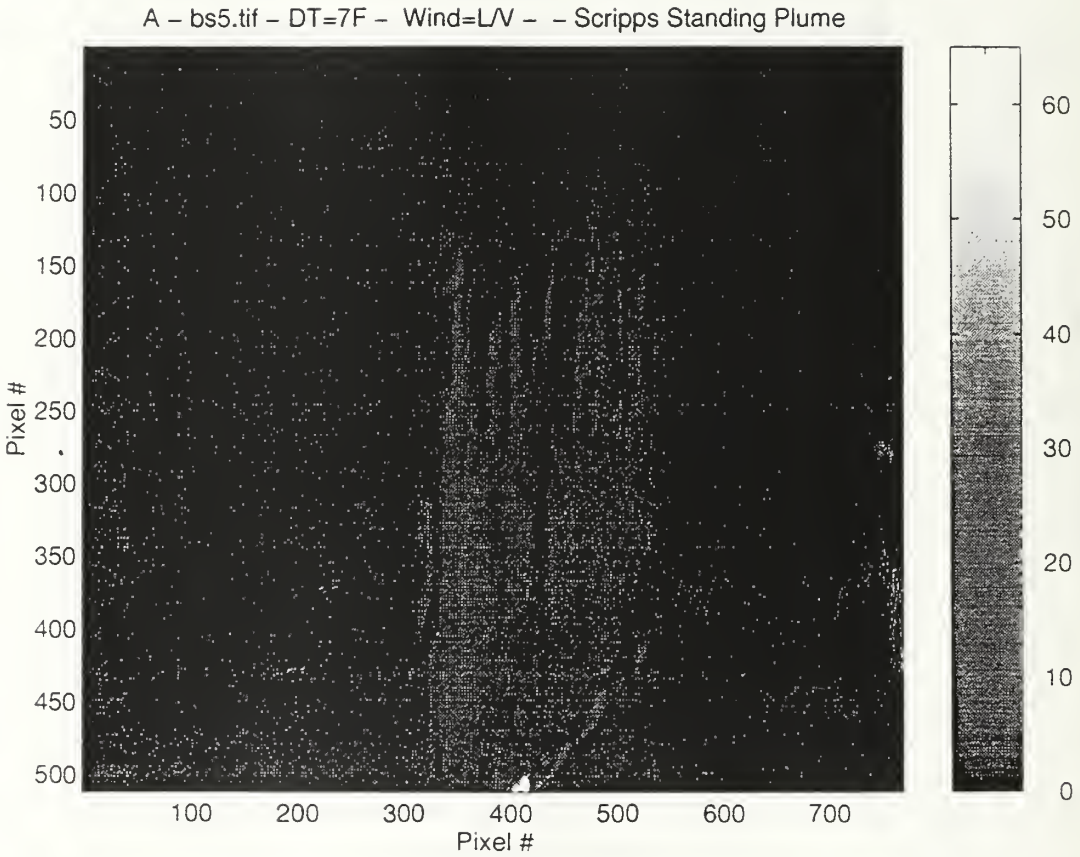

Figure 3.3a Pixel image of Scripps Pier standing plumes. Plumes are separated into well defined individual fingers extending to high heights.

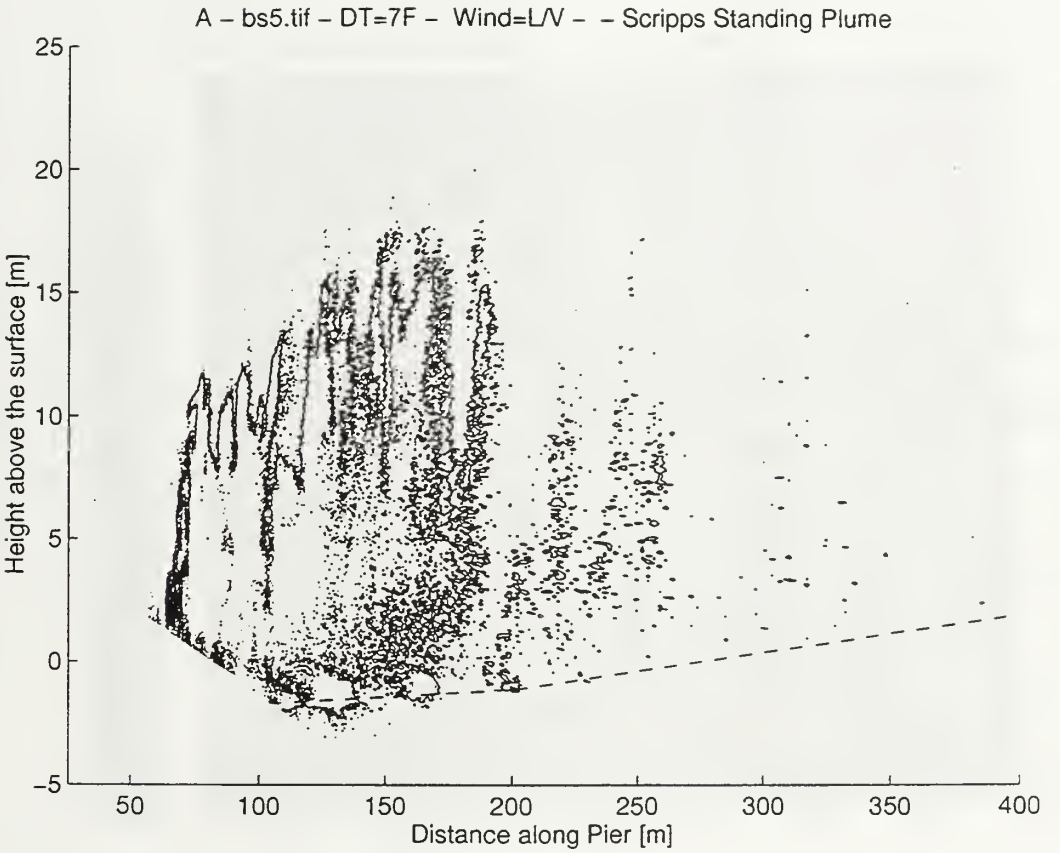

Figure 3.3b Scripps Pier standing plumes are well defined fingers developed with light and variable winds and a relatively high (sea-air) temperature difference of 7 °F. These plumes extend up to approximately 20 m and have a well defined structure, characteristic of the light wind regime.

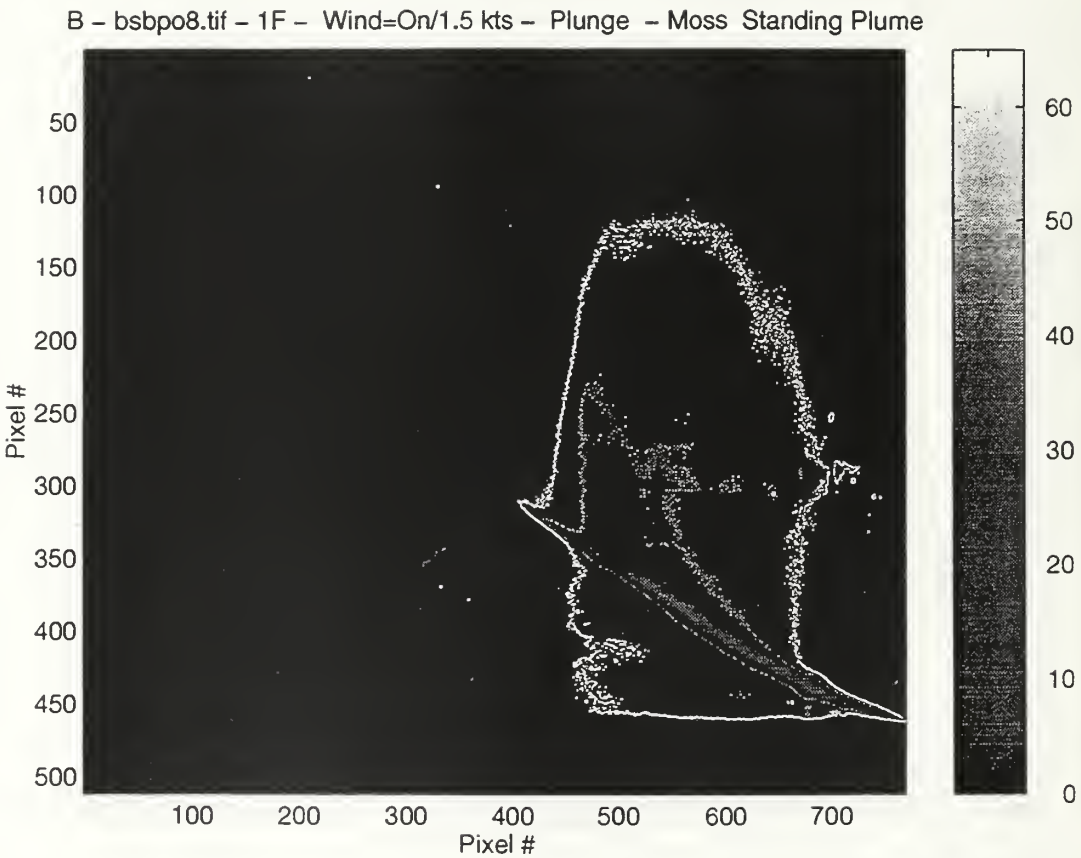

Figure 3.4a Pixel image of Moss Landing standing plume. The well defined finger structure observed in the Scripps Pier standing plumes (Figure 3.3b) are distorted by the light 1.5 kt onshore breeze.

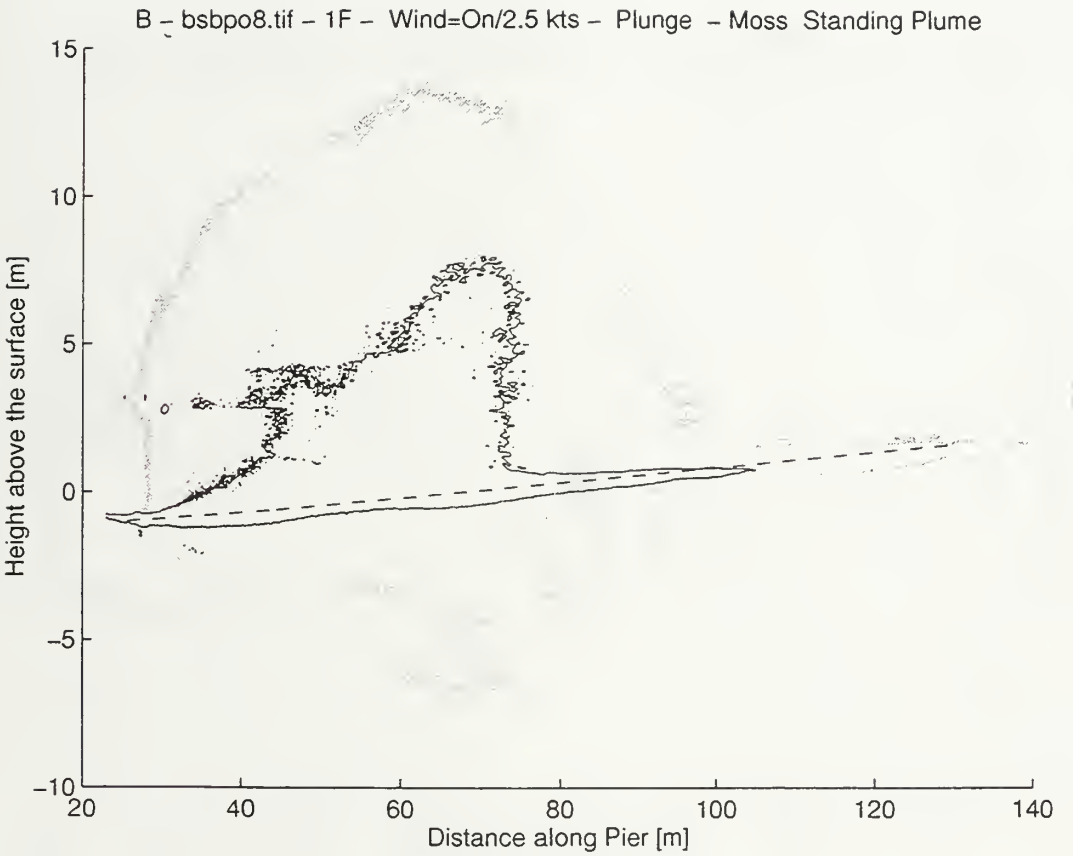

Figure 3.4b Moss Landing standing plume extends to a height of approximately 13 m and generated during high tide with 100% plunging breakers. Light breeze blends finger plumes together.

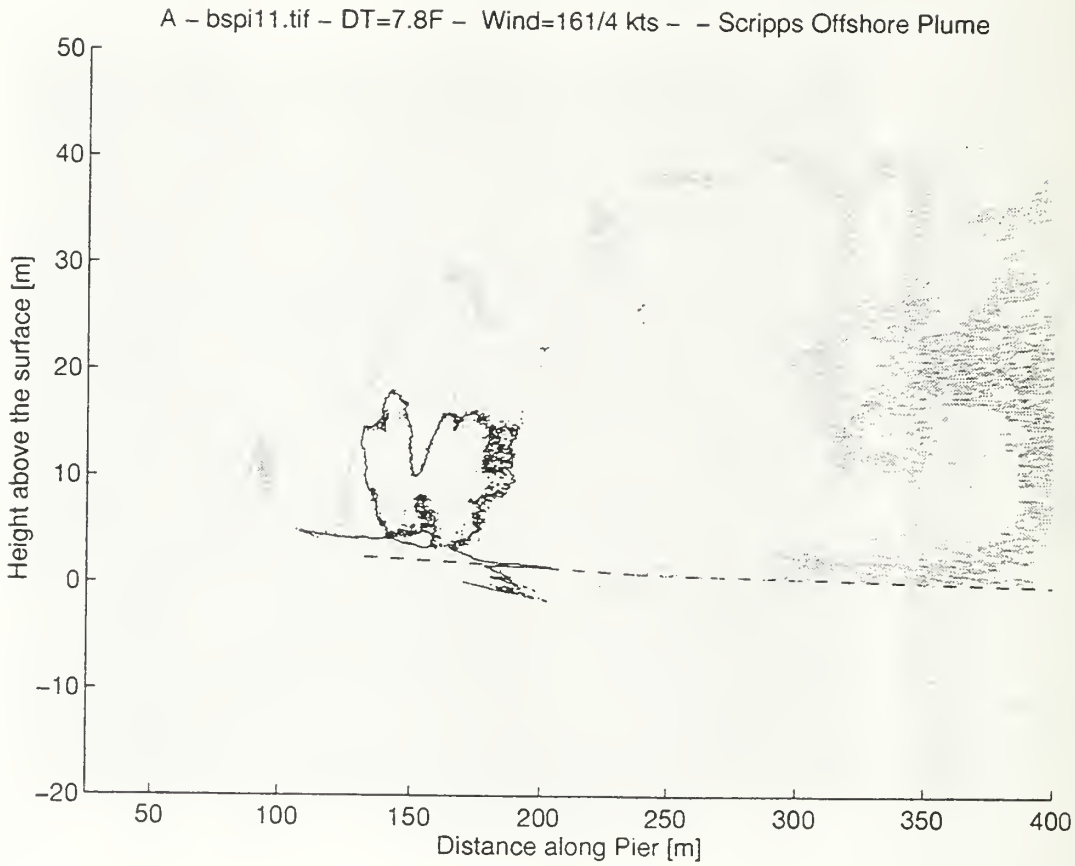

Figure 3.5 Scripps Pier off-shore plume developed with moderate off-shore wind of 4 kts and significant sea-air temperature difference of 7.8 ^{0}F. Wedge structure grows from 8-10 m near shore to near 40 m seaward.

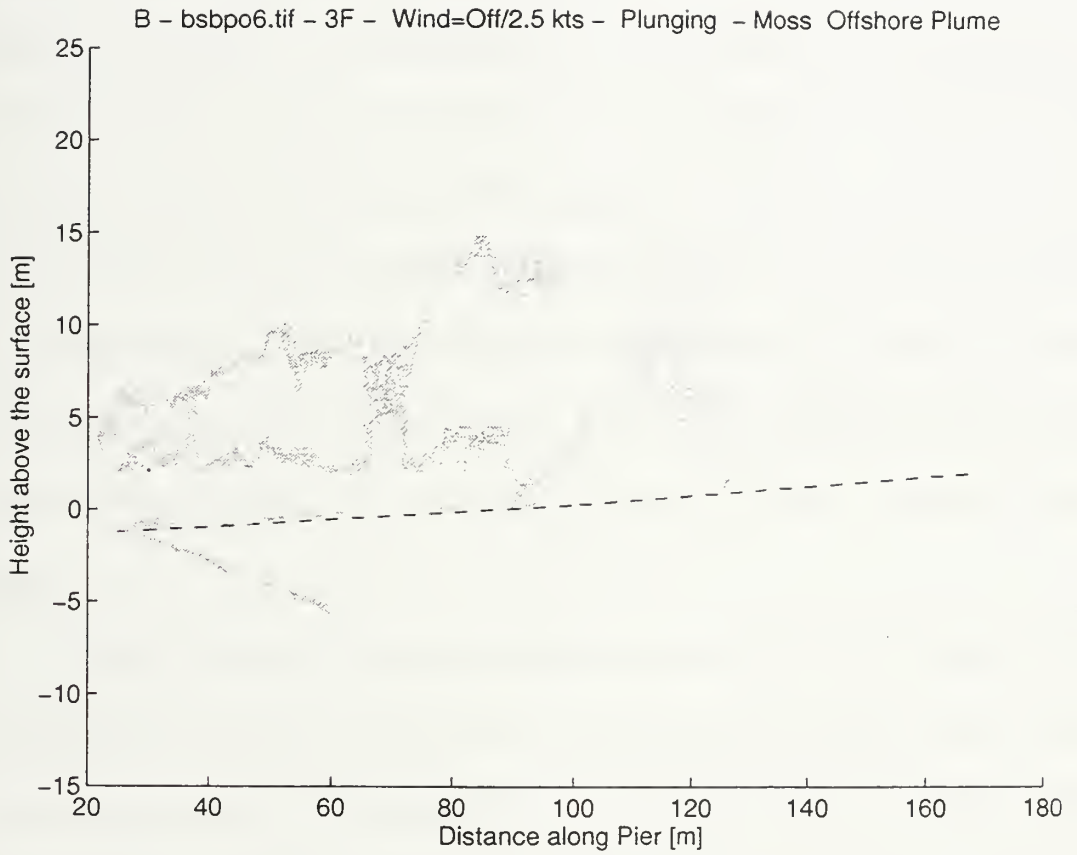

Figure 3.6 Moss Landing offshore plume generated by 2.5 kts breeze and sea-air temperature difference of 3 ^{0}F. Shoreward plume extends to 6 m and grows to 16-17 m seaward. Lighter breeze growth potential is offset by low thermal instability caused by the 3 ^{0}F temperature difference.

IV. INFLUENCING MARINE BOUNDARY LAYER PARAMETERS

A. AIR-SEA TEMPERATURE DIFFERENCES

Based on general observations of both plume structure and movement, it is apparent that several dynamic processes affect the generation and development of these surf zone aerosols. The first environmental parameter correlated to stability of the MBL is the air-sea temperature difference. At both Scripps and Moss Landing, the sea surface temperatures were greater than the overlying air temperatures. This temperature instability would generate convective mixing (upward heat flux) in the near surface air-sea boundary layer. It would be expected that the greater the difference in temperature (warm sea surface, cold air), the deeper the convective boundary layer. Thus, in the absence of any other dynamical forcing, plume development would correlate directly to the air-sea temperature difference (sea temperature greater than air temperature) resulting in taller surf-zone generated aerosol plumes.

Figure 4.1 presents a summary of plume characteristics for both experiment sites. The data were consistent in revealing that the taller plumes were more prevalent at Scripps where the greater air-sea temperature difference of 6 ^{0}F was observed. At Moss Landing, where the air-sea temperature difference was much less than at Scripps, the plume heights on average were less than half the size of the Scripps plume heights. An important consideration in comparing these plume characteristics is that the values listed are an average over hundreds of images processed for both sites. Therefore the results include varying wind regimes and breaker types in addition to air-sea temperature differences.

B. WIND REGIMES

The wind shear is closely related to the convective instability associated with the temperature differences. Wind shear produces mechanical turbulence which destroys plume vertical development. In the absence of wind (less than 2 kts), little shear exists and the convective boundary layer is more strongly influenced by the air-sea temperature differences as previously discussed. However, with winds greater than 3 kts, wind shear produced mechanical turbulence has an impact on the plume structure and development. This is most apparent with an off shore wind when the off shore wedge plume structure is developed. Near the surface in the breaker zone strong unstable shear cells are developed by the off-shore winds opposing the incoming wave trains and breakers. This strong area of shear instability decreases rapidly with height, as the dry terrestrial air mixes and evaporates the plume edge as the newly generated aerosols are advected seaward. The strongest shear is concentrated near the surface and decreases rapidly with height.

At low wind speeds, convective development of the plume seems to be slightly dampened as the near surface wind shear zone appears broad. But as wind speed increases, convective development is severely dampened as the shear zone becomes narrow and more concentrated. As observed during the transition between the land breeze and sea breeze, tall convective standing plumes are formed in the calm winds associated with the transition period between the wind regimes. As the land breeze develops and winds increase, the overall height and orientation of the plumes changes into an off-shore wedge. As winds continue to increase, the plume heights continue to decrease.

Results in Figure 4.1 are somewhat misleading in view of the possible wind

speed/plume height correlation. As with air-sea temperature differences, it would be expected that the site with the largest winds would have the smallest plumes. In the case of wind, the land/sea breeze wind regimes observed in San Diego are much stronger than those observed in Moss Landing. This would mean that the standing plumes developed within the transition window in San Diego, should be much taller than those at Moss Landing. Also, as the land/sea breeze became stronger in San Diego, the plumes did decrease, but because they were higher to begin with, due to convective instability, they were still taller than the plumes at Moss Landing.

C. BULK RICHARDSON NUMBER RELATIONSHIP

The observation of plume dependence on temperature difference and wind speed can be related to a parameter used to describe thermal stability, the Bulk Richardson Number (R_B) (Stull, 1988). R_B is a dimensionless number that describes the proclivity to develop turbulence (Pond, Pickard, 1991).

$$\mathbf{R_B} = \frac{g\ \Delta\overline{\theta}_v\ \Delta z}{\Delta\overline{\theta}_v\ [(\Delta\overline{U})^2+(\Delta\overline{V})^2]}$$

Where: g = acceleration due to gravity.
$\Delta\theta_v$ = virtual potential temperature
Δz = height above local terrain
ΔU = eastward wind component
ΔV = northward wind component

R_B as a parameter is based in the fact that buoyant produced turbulence is proportioned to the air-sea temperature differences and inversely proportional to the wind shear. As the sea surface becomes warmer than the overlying air, turbulence will increase. Subsequently, it also relates turbulence to wind shear/speed. It describes buoyant turbulence to be inversely proportional to the square of the wind speed. This sensitivity to wind means that a small increase in velocity will result in a large decrease in turbulence.

D. INSTABILITY DATA

There were 15 successful measurement days for the two experimental sites with 56 hours of data analyzed. Now detailed descriptions of 5 individual days will be presented and discussed. Figure 4.2 depicts an interesting combination of the impact of air-sea temperature difference and the wind speed on average plume heights at Moss Landing. At the beginning of the period, the air-sea temperature difference was negligible, increasing to almost 3 °F by the end of the period. The overall plume height trend increased during this period. Similarly, the two wind speed minima correlate to two plume height peaks. Results in Figure 4.3 from Moss Landing describe occurrences during an evening with little fluctuation of the air-sea temperature difference, but shows an interesting relationship of wind speed and maximum plume height. Again, maximum winds yield minimum plume height, and minimum winds produce maximum plume height.

Figure 4.4 from Moss Landing shows data taken during brisk on-shore winds associated with a tight pressure gradient forced by a synoptic scale weak cold front that had passed over the Monterey Peninsula earlier that day. The most interesting trend in this noisy data set is that the winds persist at speeds greater than 3 kts. Throughout the evening plume

heights decreased over time, except after 2200 hours when the air-sea temperature difference started to increase. This increase in temperature difference appears to produce an increase in plume height under somewhat sustained winds. This data appears to exemplify the delicate balance between wind speed and air-sea temperature differences in the development of these plumes.

Results in Figure 4.5 from Scripps Pier illustrate that larger temperature differences are associated with the higher plume heights. In this example, as wind speed increased, a resulting decrease of maximum plume height occurred. Additionally, there appears to be a correlation between wind speed and variability of the plume height. At lower wind speeds, the variance of the five plume heights is less, similar to what would be expected for a uniform standing plume structure. As wind speed increases, greater variance in the plume height is observed, possibly suggesting a feature similar to an off-shore wedge plume structure.

Figure 4.6 from the Scripps Pier again shows the inverse correlation between wind speed and plume height. Similar to Figure 4.5, the variance in the plume height structure decreases with decreasing wind speed, again possibly suggesting the formation of a more uniform plume structure such as the standing plume.

E. BREAKER TYPE

The last critical ingredient in the generation and development of surf zone aerosol plumes is also the most unpredictable. As described in Chapter II, the breaker type has a direct link to the development of the plume. A plunging breaker will create a large number of bubbles.

During EOPACE I and II, no direct surf zone wave measurements were made that

could be used for direct correlation of breaker type and plume height. However, by assuming that the surf would have more of a plunging characteristic during high tide, simple tidal observations were added to the data analysis with some interesting results.

Results in Figures 4.7 and 4.8 are from periods at Moss Landing where a large tidal variation was interfaced with a steep beach face at high tide. In both figures, the plume heights increases as the tide rises. Figure 4.9 shows the contrast to the rising tide seen in the previous figures. In this case the tide is receding whereas the expected transition would be from plunging breakers to more spilling breakers. In this example, the wind is negligible and as the tide moves out, the plume height decreases.

Results in Figure 4.10 from Scripps Pier illustrates that with minimal tidal range, or reduced surf zone activity, this element of plume generation has a minimal impact as compared to the temperature and wind speed parameters.

Location	Moss Landing Pier	Scripp's Pier
Sea - Air Temperature	3 ° F	6 ° F
Wind Speed	2 kts	6 kts
Average Plume Height	9.5 meters	24.7 meters

Figure 4.1 Summary of plume characterisitcs for Moss Landing and Scripp's pier.

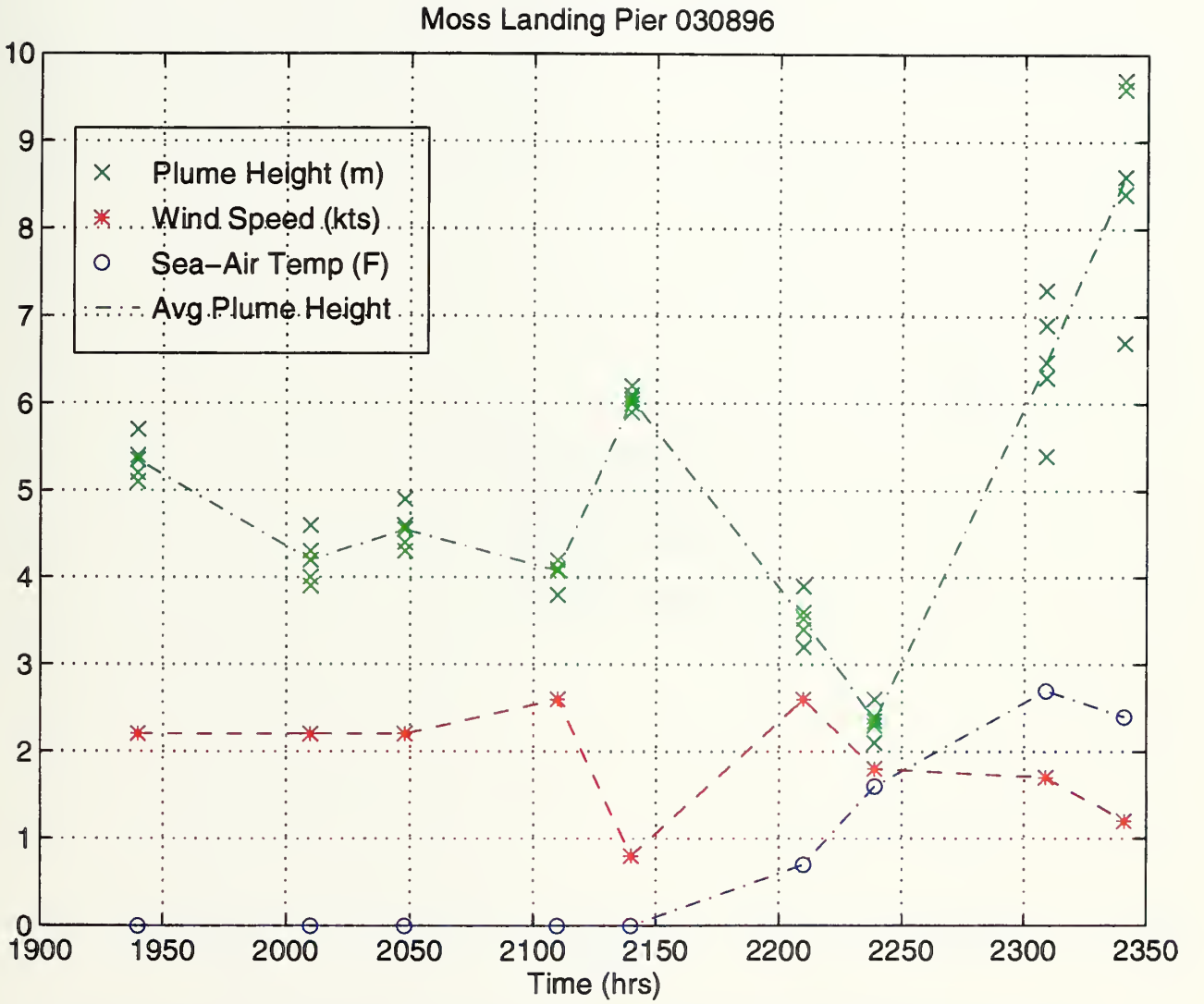

Figure 4.2 Moss Landing Pier data for 030896. This noisy data is somewhat misleading when focusing on the correlation between wind speed and plume height. However, in the mid to late period as wind speed decreases, plume height increases as would be expected.

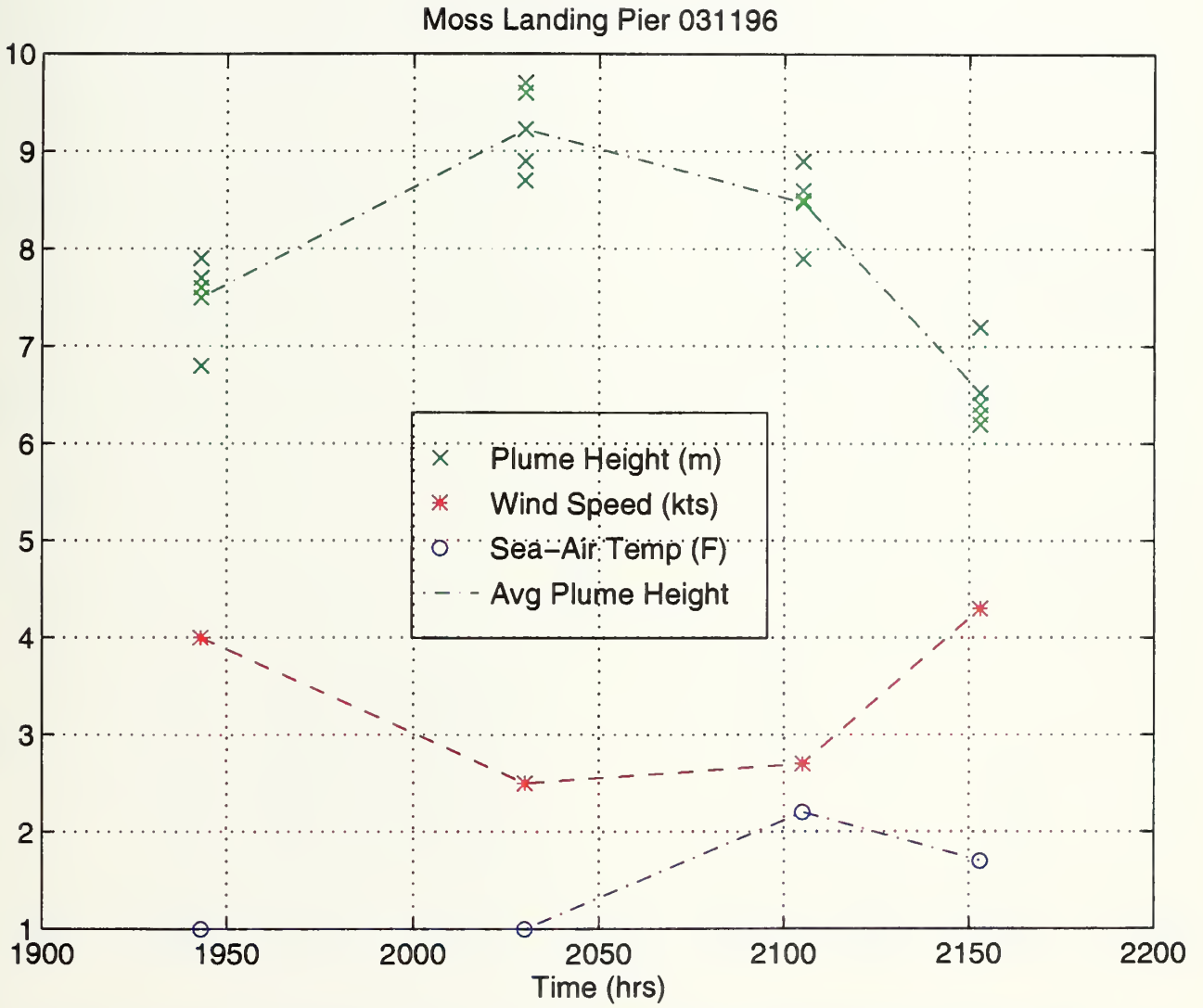

Figure 4.3 Moss Landing Pier data for 031196. The temperature difference for this evening were minimal. Plume height appears much more sensitive to wind speed variations.

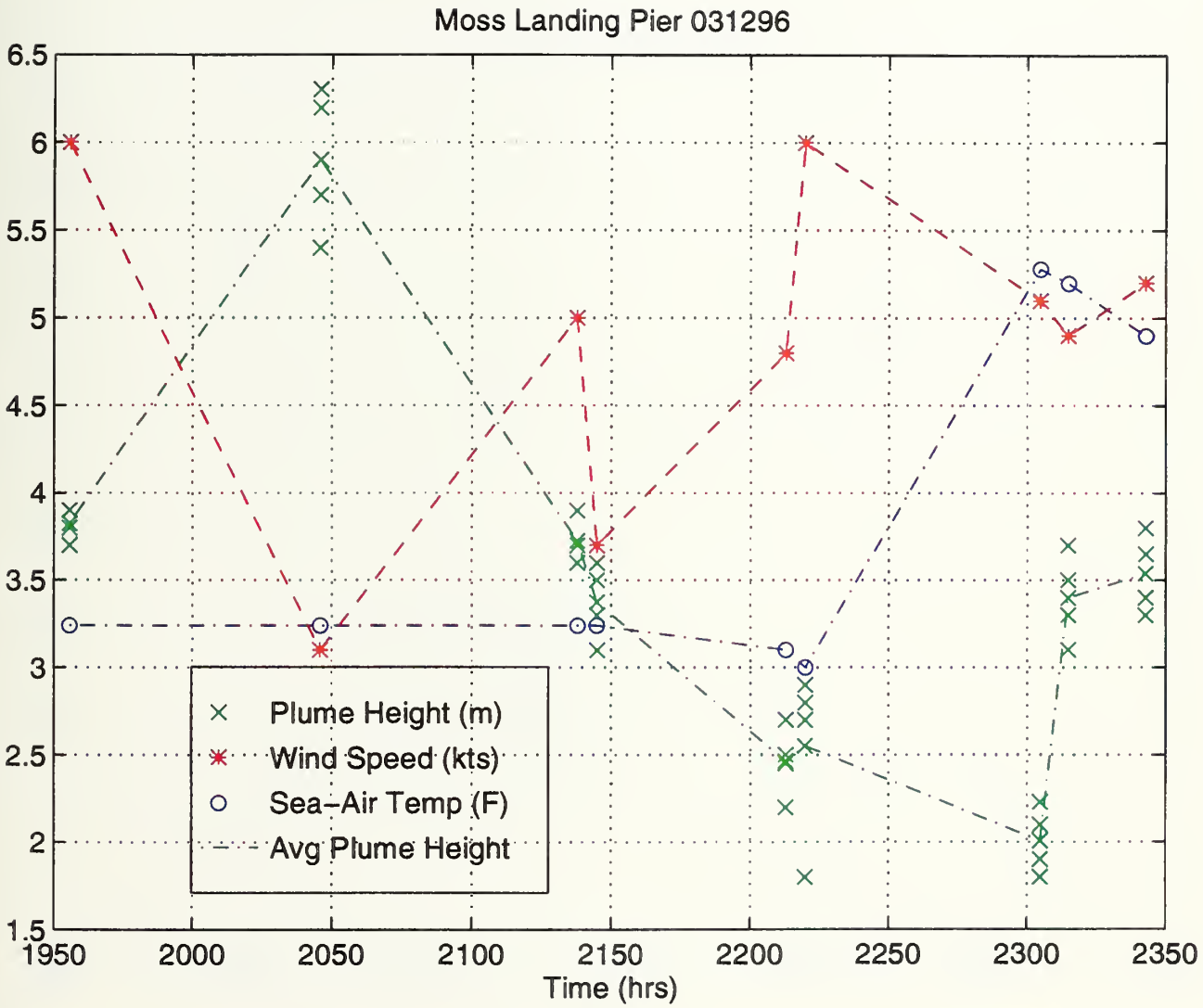

Figure 4.4 Moss Landing Pier data for 031296. A tightened synoptic pressure gradient has created a strong on-shore flow throughout the evening. As winds persist above 3 kts, plume heights gradually decrease.

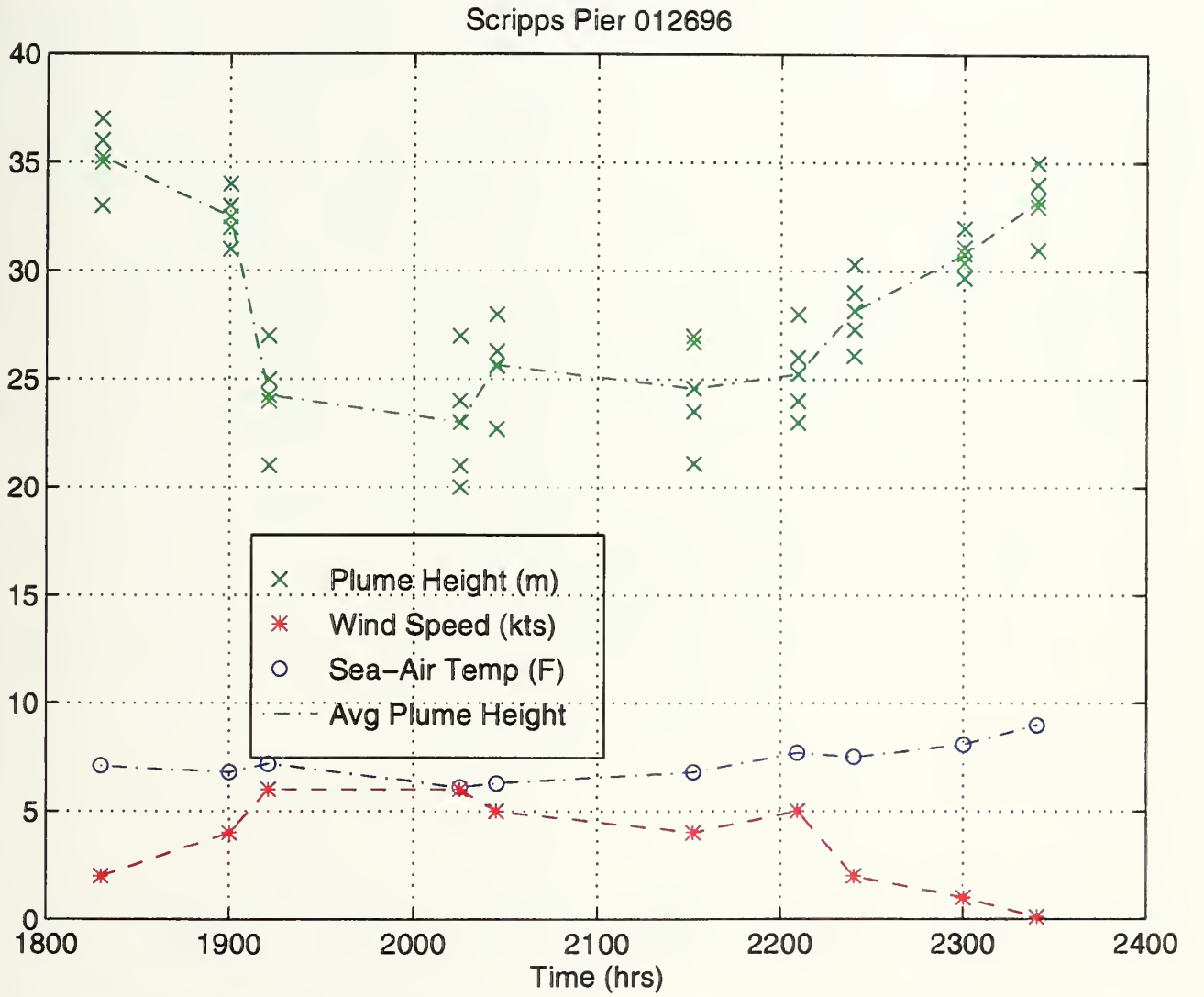

Figure 4.5 Scripps Pier data for 012696. An excellent example of the influence of wind speed on plume height. Of significance is the large temperature difference and taller plumes associated with the Scripps data.

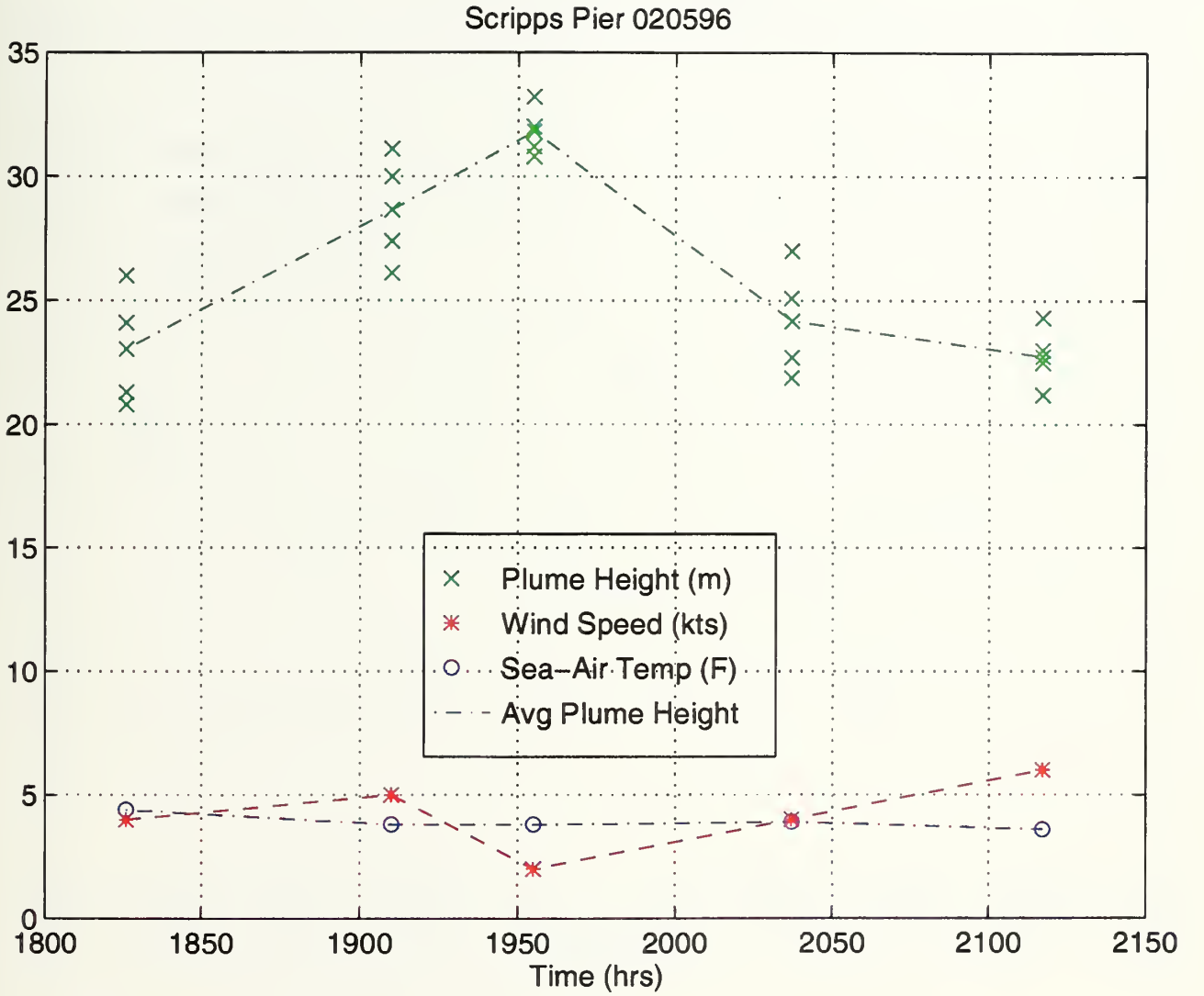

Figure 4.6 Scripps Pier data for 020596. Notice as winds decrease, the variance of the plume heights decrease. This indicates the formation of a more uniform plume structure, similar to standing plumes.

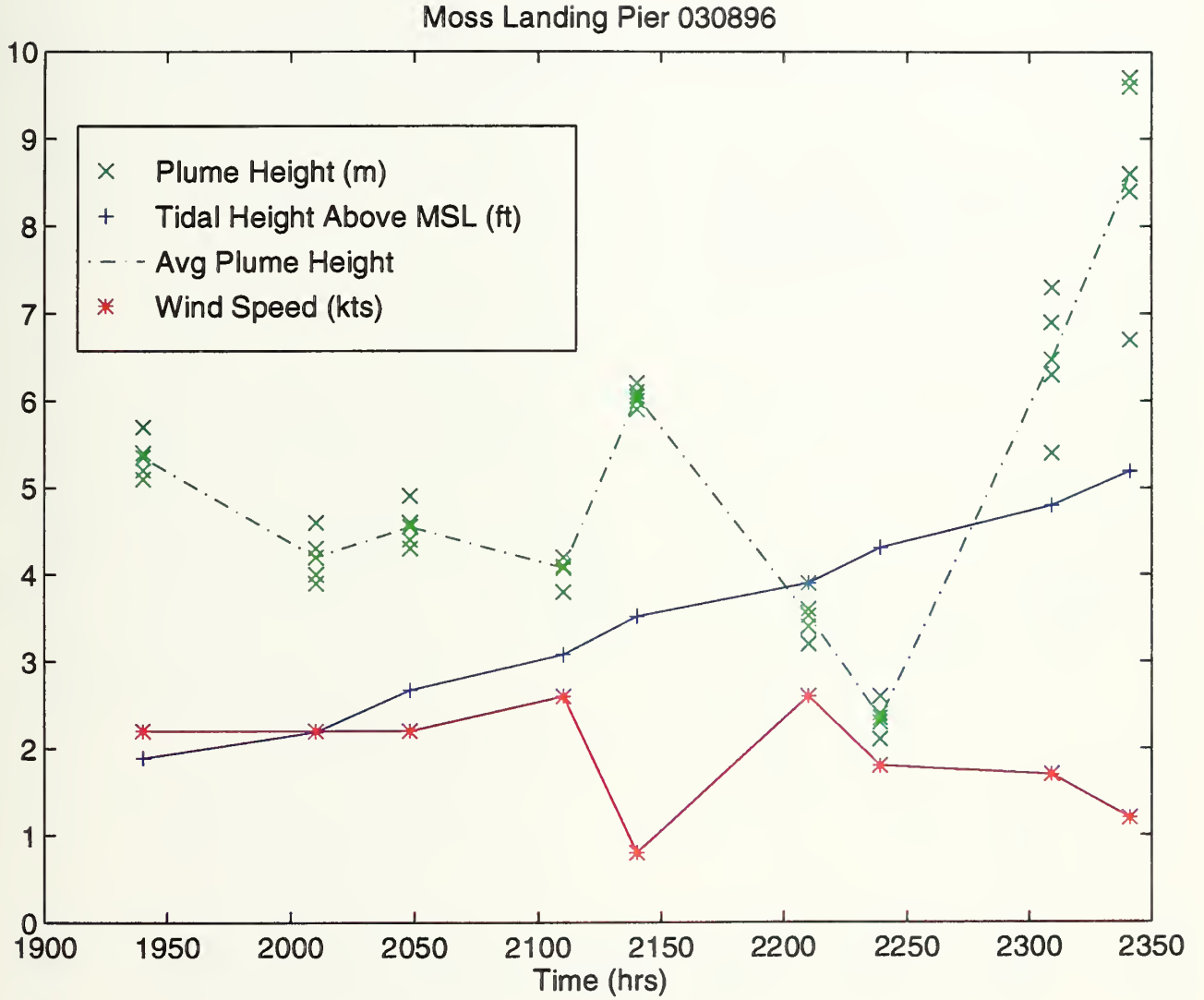

Figure 4.7 Moss Landing Pier data for 030896. Strong correlation between incoming tide on a steep beach face creating plunging breakers. The plunging breakers combined with decreasing wind speeds allow the plumes to grow to greater heights over time.

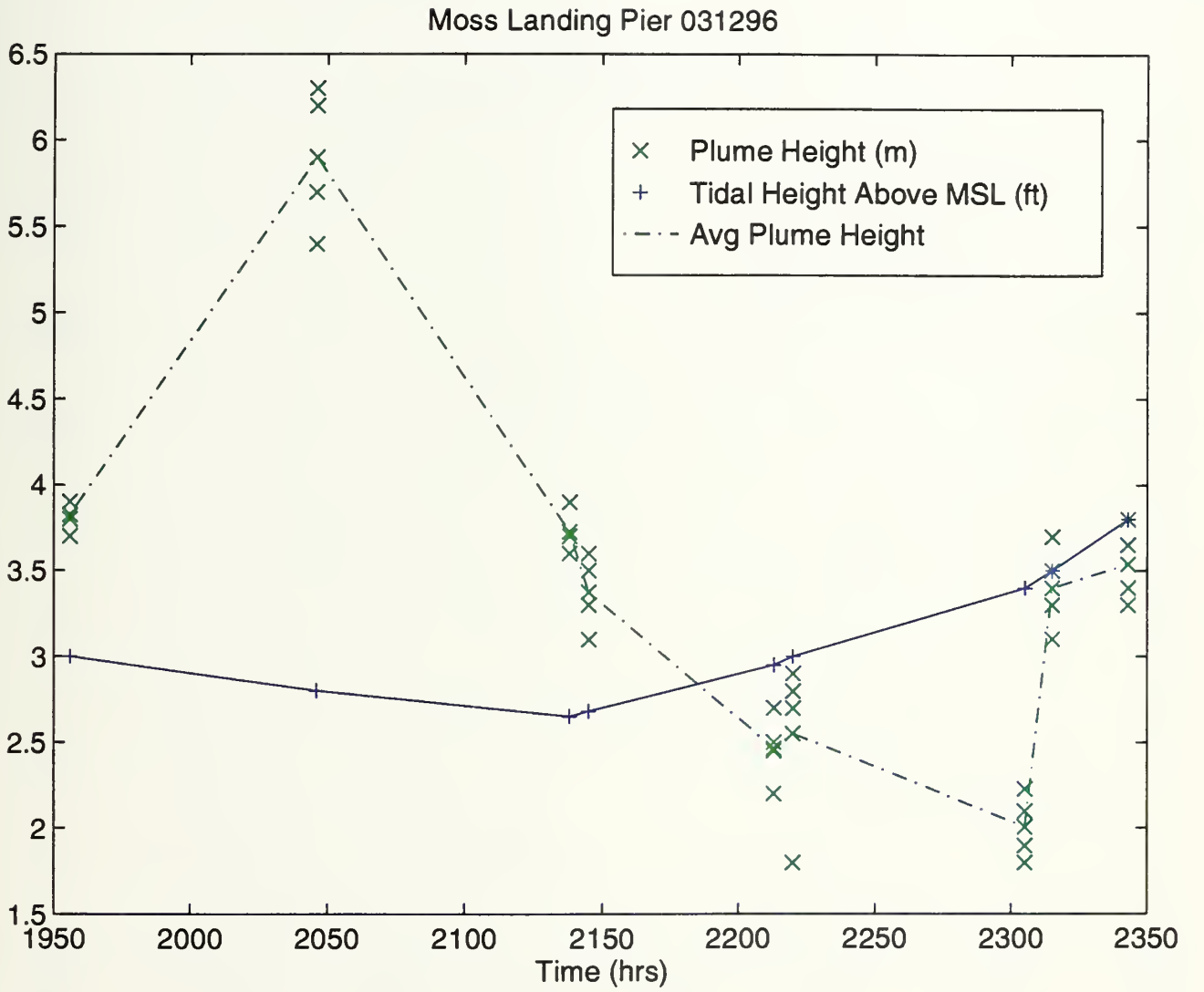

Figure 4.8 Moss Landing Pier data for 0301296. All parameters influence this noisy data set that is dominated by strong on-shore flow. As winds decrease after 2300, the influence of the decreased winds and rising tide combine to produce rising plumes.

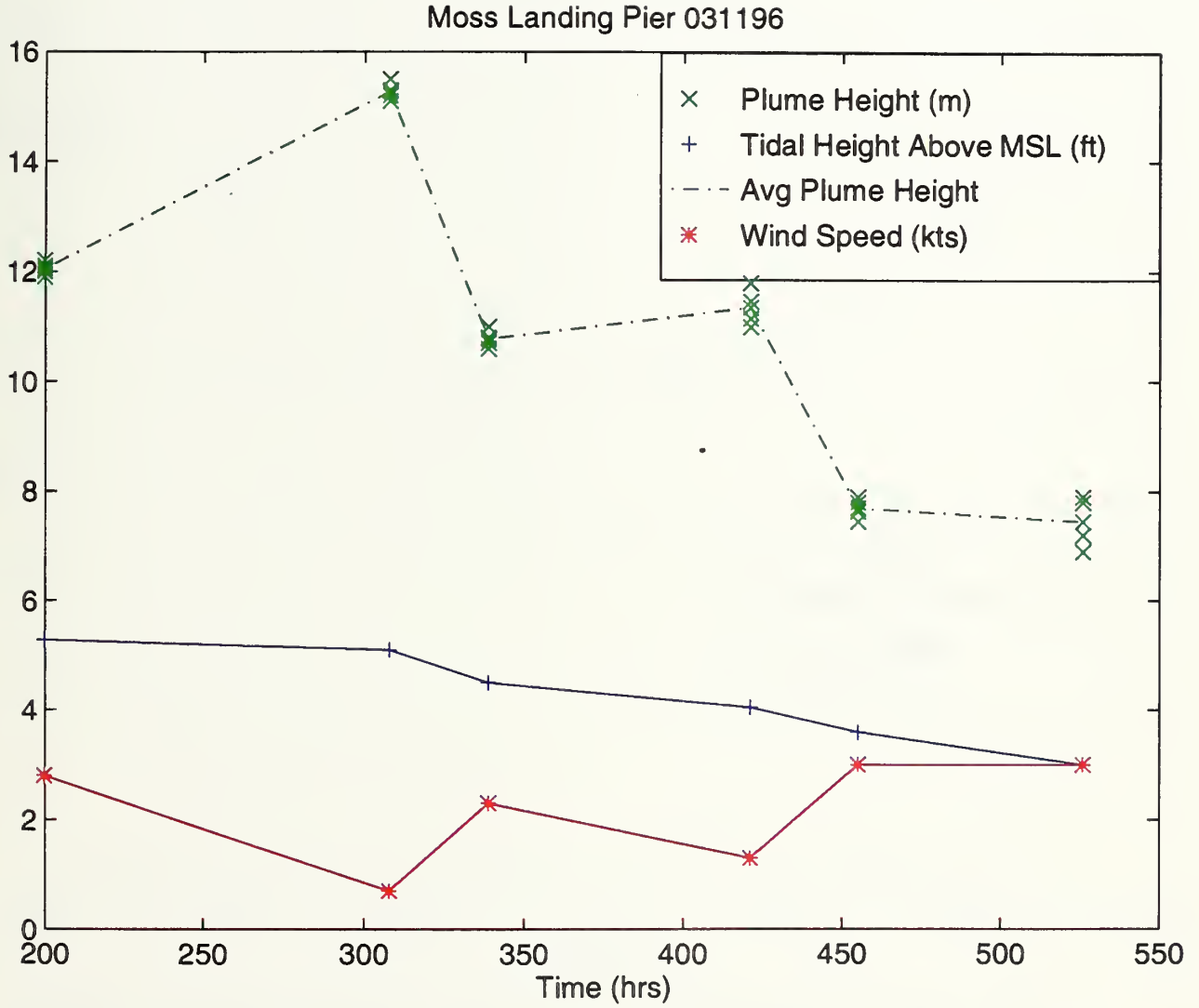

Figure 4.9 Moss Landing Pier data for 031196. In this example, it is a combination of increasing winds and outgoing tides that result in the decreasing plume heights.

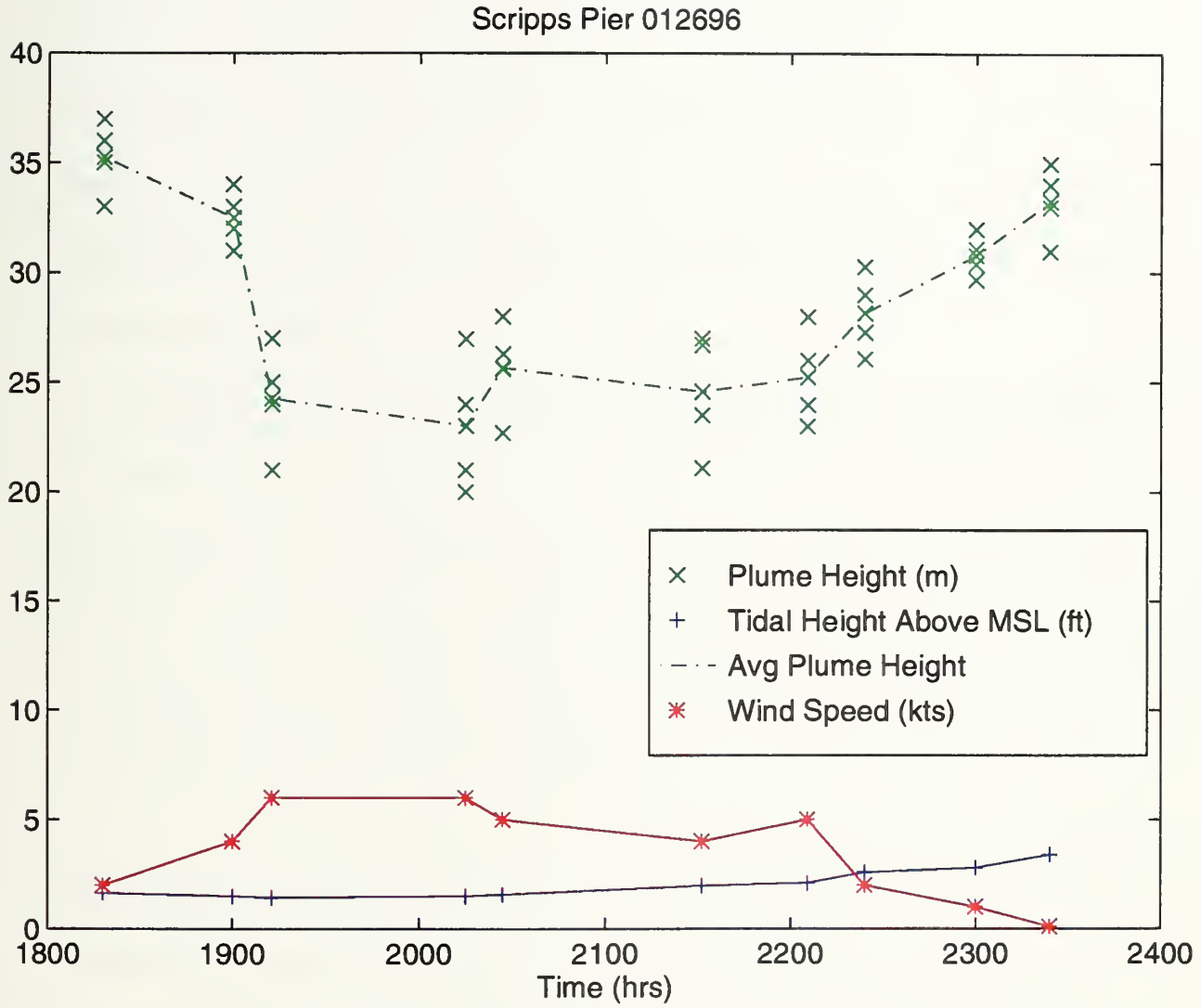

Figure 4.10 Scripps Pier data for 012696. The small tidal range characteristic of San Diego has little contributing impact on plume development. The influences of wind speed and temperature difference are dominant.

V. TRANSMISSION OBSERVATIONS DURING EOPACE I

Transmission measurements near FLIR wavelengths (3.5 and 10.6 μm) were recorded across the surf zone by a group at NRaD headed by Rowena Carlson, during the Scripps Pier EOPACE I experiment. These data are one of the first which show the impact on IR systems with an optical path within the surf aerosol generation region. These transmission data quantify the potential impact of the surf zone generated aerosols. Preliminary results indicate a signal degradation of up to 35 percent while looking across the surf under certain environmental conditions.

Transmittance was measured across the surf zone at a height of 5 m. Environmental data to include wind speed and direction were also recorded at the black body source and the receiver. Figures 5.1 and 5.2 give representative data during the experiment period for early morning and evening time periods, respectively. The top graph in each figure shows wind speed represented as the solid line referenced on the left margin, and wind direction as squares averaged over 5 minute intervals and referenced to the right margin. The lower graph represents total transmittance along the optical path from the source on the beach to the receiver on the pier seaward of the breaker zone. This graph highlights the impact of surf zone aerosols on transmission at the 3.5μm and 10.6μm wavelengths. These wavelengths are used by the Navy's EO systems such as FLIR. Since system alignment problems can create up to a 10 percent transmittance error, the 10.6μm transmittance values may exceed 100 percent.

These results agree with previously discussed factors affecting aerosol plumes. A very weak synoptic weather pattern prevailed over Southern California 29 January to 2

February 1996. This allowed mesoscale wind field development caused by differential heating of the adjacent land/sea areas. As seen in Figure 5.1, through the early morning hours up to approximately 0915, the land breeze was dominant. Transmittance during this same time frame was high, greater than 90% for both 3.5 and 10.6μm. The tide was low at the beginning of the period and gradually built towards mean water with mostly spilling breakers. From 0915 through 1015 the wind backed westerly, corresponding to the transition from land breeze to sea breeze. During this transition period the wind becomes calm and transmission is degraded in both wavelengths 13-15 percent. The decrease in transmission could have been a result of standing aerosol plumes being created in the surf area, injecting a higher concentration of aerosols along the optical path over the surf zone. As the sea breeze establishes itself and the wind speed increases, transmittance also increases and resumes previous levels. This agrees with the formation of the off-shore wedge decreasing the aerosol concentration along the optical path. It is also observed that as the tide increases, creating a larger number of plunging breakers, that the transmittance does not return to its origin values of high transmittance. As mentioned previously, plunging breakers inject aerosols higher into the ITBL due to higher vertical velocities at their formation.

The sea breeze transitioning into land breeze is evident in the time series of Figure 5.2. From early afternoon through 1800 on 2 February the transmittance was high (95 to greater than 100%). This was associated with a 5 knot sea breeze and primarily spilling breakers in the surf zone during low tide. In the transition period from 1900 to 2015, the winds veered from westerly to easterly and were relatively calm. Correspondingly, the transmittance decreased 5-8 percent at 10.6μm and 20-30 percent at 3.5μm and continued

to be degraded by 5-7 percent less than its original value before the shift in wind regimes. Again, this closely corresponds to an increase in the number of plunging breakers and high tide at 2100.

Laser Scattering data were also available during these periods so plume features can also be examined. A comparison of average plume height and wind speed (Figure 5.3), shows the maximum plume development occurs during the land-sea breeze transition up to 28 m. Of note is the variance of the plumes. During the calm transitional winds the plumes are relatively uniform in height, (Figures 5.4 and 5.5) and have the appearance of standing plumes. As the wind increases the sampled plume heights become more unstable, similar to a wedge type plume structure.

From this data it appears that transmittance closely relates to the wind influenced plume structure. During the transition from land/sea or sea/land breeze, standing plumes develop creating a higher concentration of aerosols along the optical path over the surf area. The tidal period (Figure 5.6) and breaker type also contribute to the structure and diversity of the plumes with predominant plunging breakers at high tide inducing more aerosols (greater quantity of trapped air) with higher injection speeds within the surf zone region. The stability of the IBL also dictates the vertical development of these plumes. The more unstable the IBL is, the greater vertical height these plumes will achieve. As the IBL becomes more stable, the greater the aerosols will be retarded in their convective development.

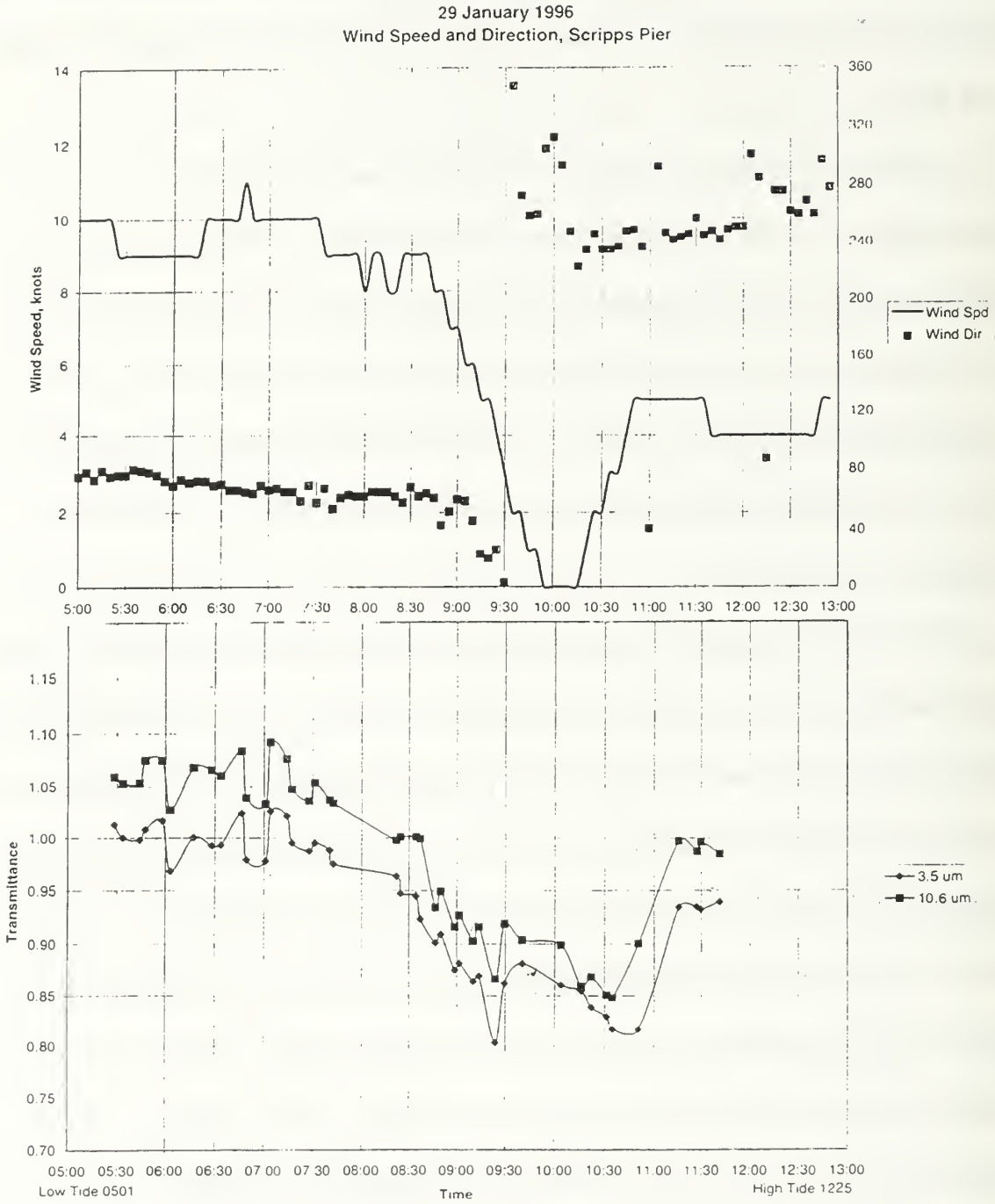

Figure 5.1 Scripps Pier transmittance data for daytime hours 29 January 1996. The minimum in transmittance data corresponds to the calm transition period between the land and sea breezes. This calm period would be conducive to the generation of tall standing plumes within the surf zone. (From Carlson, 1996)

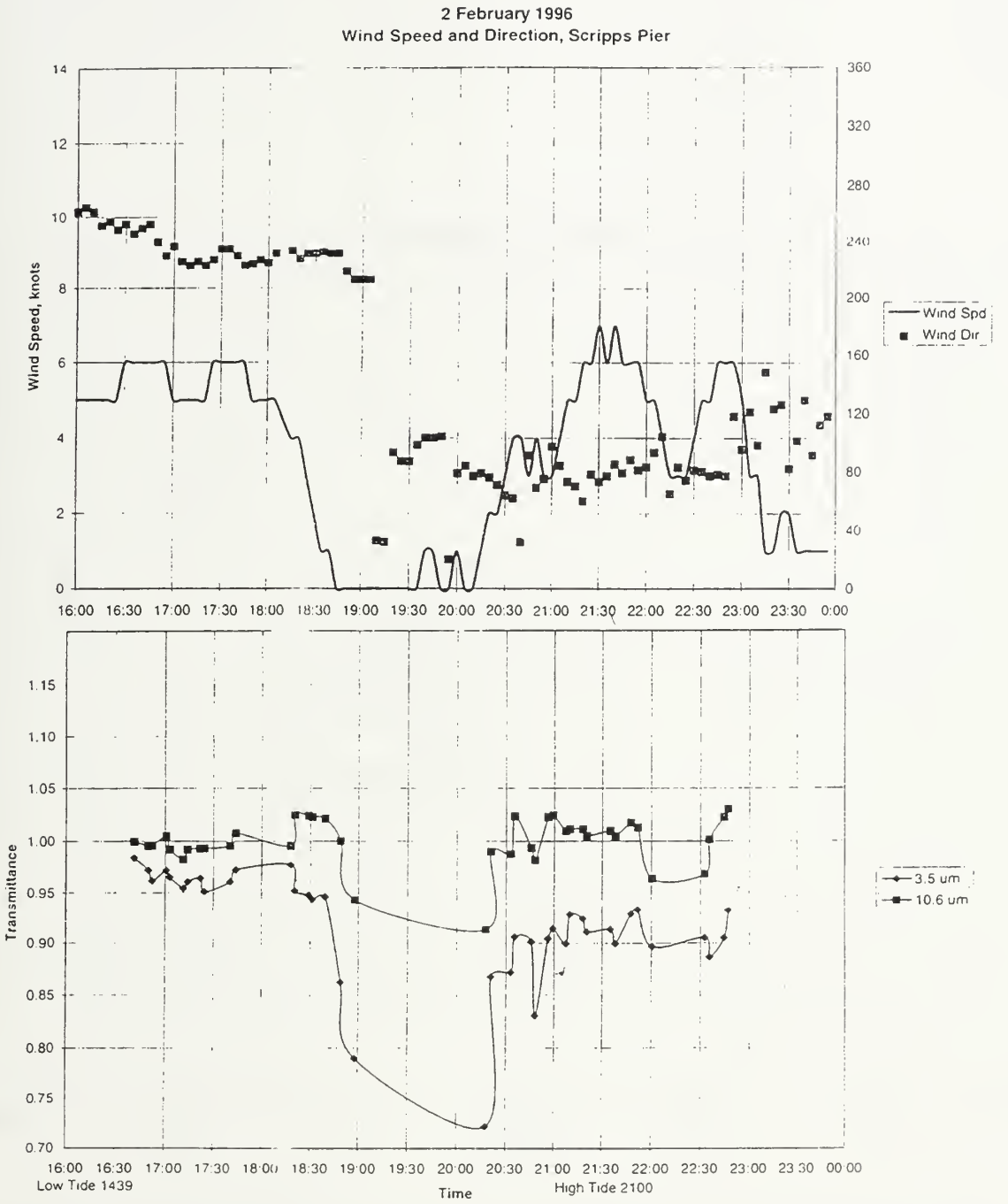

Figure 5.2 Scripps Pier transmittance data for evening hours 2 February 1996. Minimum in transmittance correlates to transition period of land and sea breezes. Standing plumes were observed (Figure 5.4) during this time period. (From Carlson, 1996)

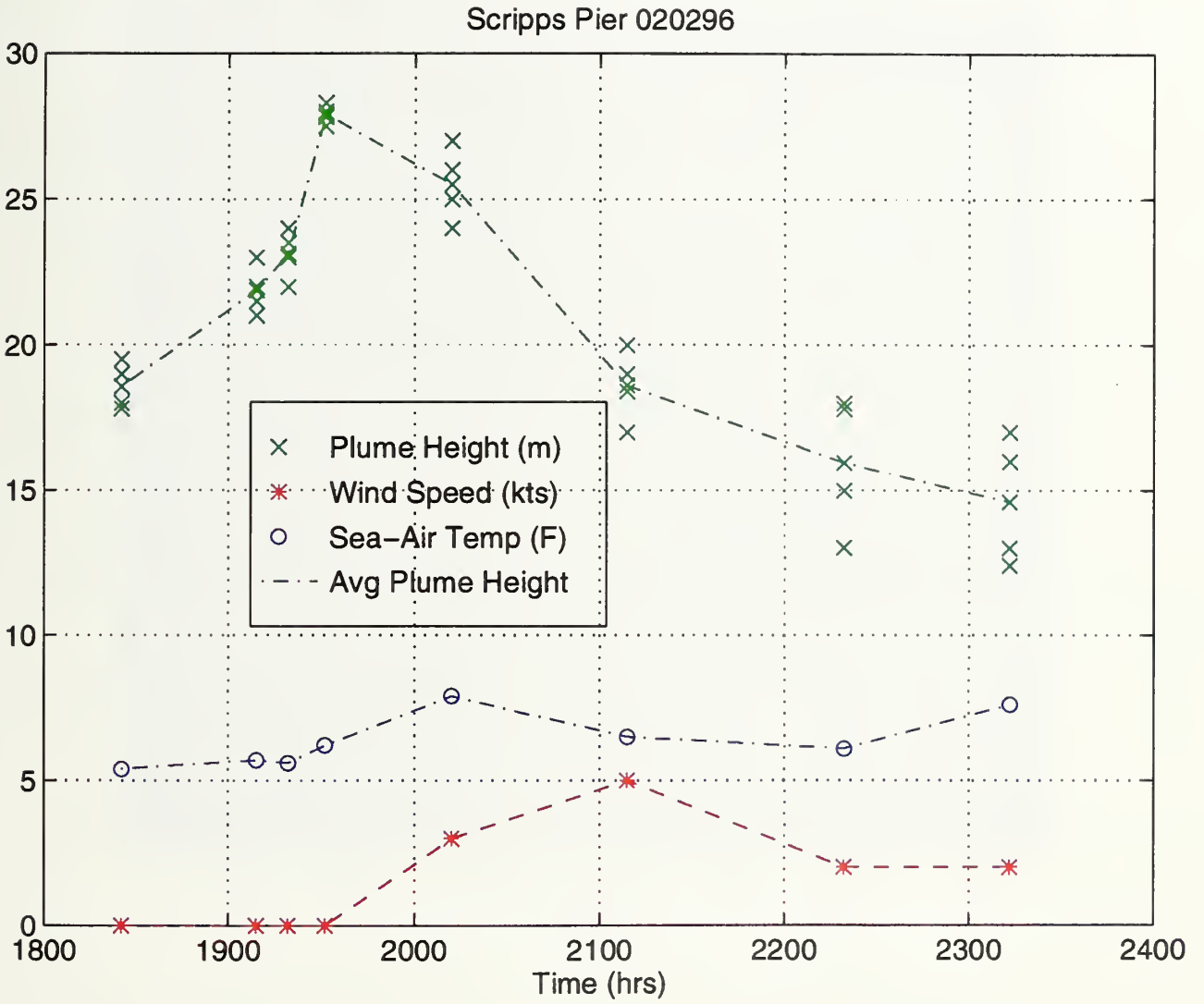

Figure 5.3 Scripps Pier data for 020296. Early observations indicate development of tall standing plumes. As wind speed increases, a corresponding decrease in plume height and increase in plume variability develop.

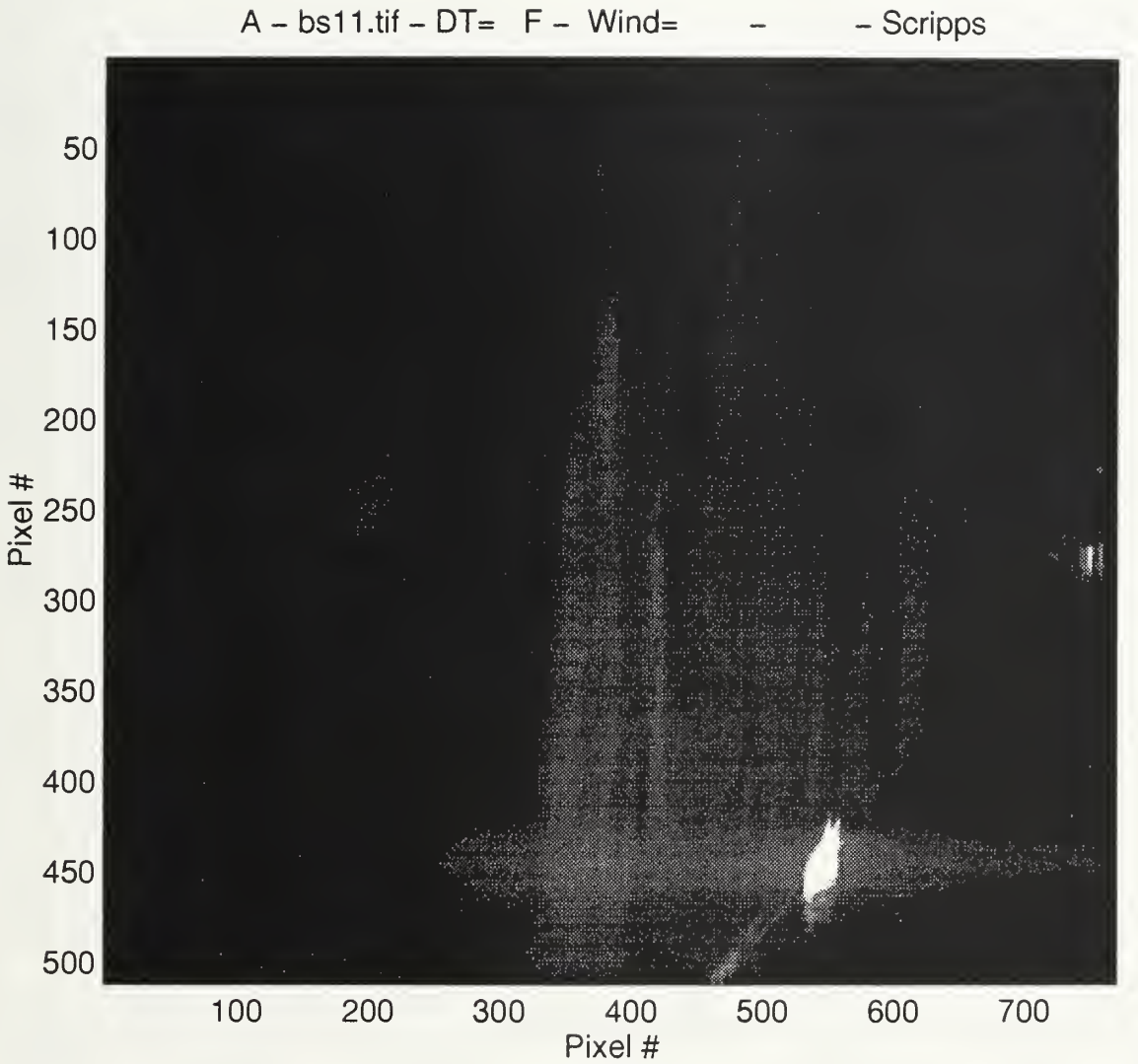

Figure 5.4 Raw data image of Scripps Pier standing plumes during land-sea breeze transition 020296.

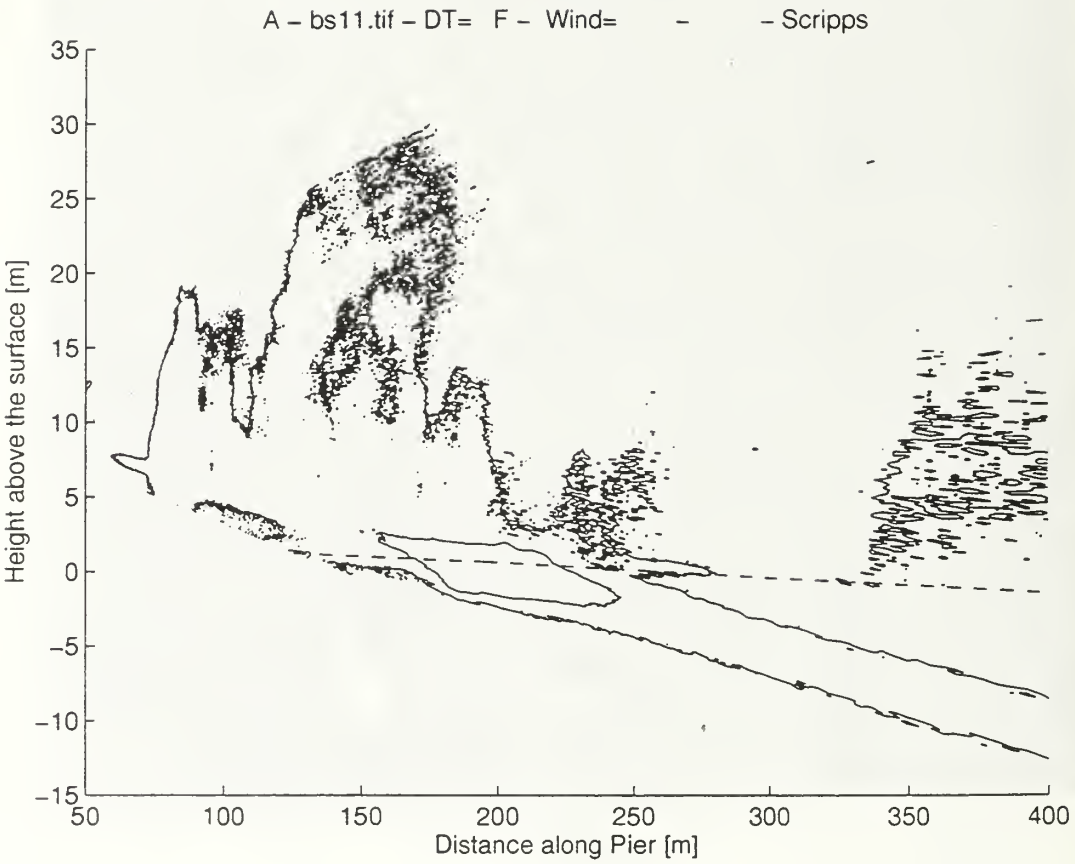

Figure 5.5 Processed image of Scripps Pier standing plume during the transition of the land-sea breeze 020296.

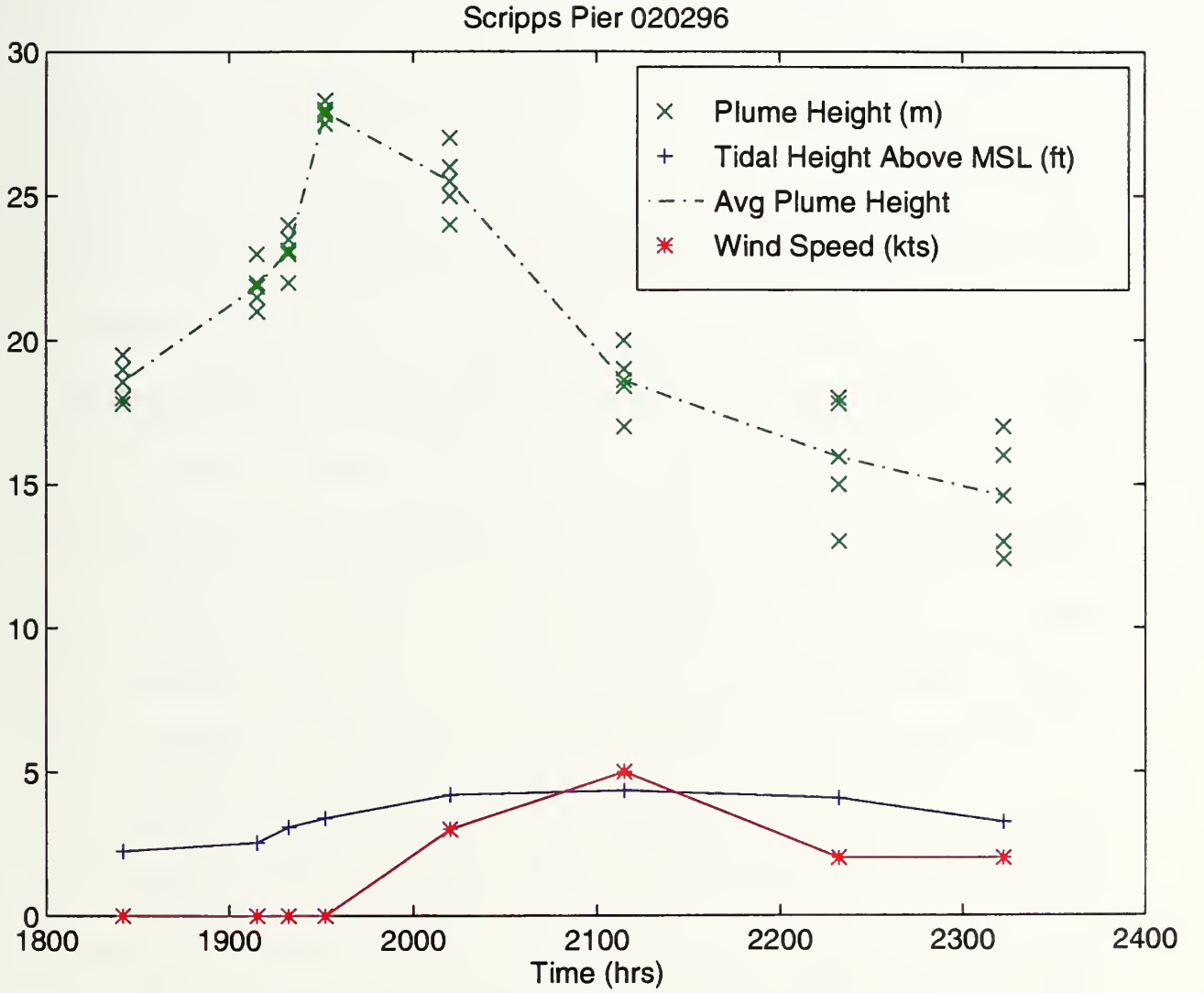

Figure 5.6 Scripps Pier plume height and tidal data for 020296. Minimal tidal variations associated with Scripps may indicate that plumes are more dependent on wind speed variations and temperature differences than breaker type for their development and structure.

VI. CONCLUSIONS/RECOMMENDATIONS

The primary objective of the EOPACE experiment series was to quantify the effects on EO propagation across the surf zone created by surf generated aerosols. From Carlson's data it is obvious that present EO systems can be degraded up to 35 percent while looking across the surf under certain environmental conditions. In evaluation of the surf generated aerosol plumes, it was observed that in light wind regimes with the water temperatures greater than the air and dynamic surf activity (plunging breaker with high tide) that the concentration and structure of the plumes were at their peak. This peak in plume generation similarly corresponded in the maximum degradation in the IR transmittance observed during EOPACE Phase I. The ability to determine conditions conducive to peak aerosol formation are essential in tactical employment of military EO systems within the coastal environment.

Degradation of IR sensors within the surf is a new phenomenon and no guidelines exist to predict the formation and concentration of responsible aerosol plumes. During the Moss Landing phase of EOPACE, the following basic forecasting indicators were used to determine the plume structures to a high degree of accuracy. The greatest scattering of the laser source was observed with light winds (less than 2 knots) and the generation of the standing plume structure. As observed in the Scripps Pier data, transmittance can be reduced up to an hour on either side of the sea/land breeze transition window. For these mesoscale thermally driven winds to form, a weak synoptic pattern and sufficient differential heating is required. Standing plumes are also influenced by the tidal period and breaker type, with plunging breakers providing the greatest aerosol source for these type of plumes. Finally as

a function of stability, the greater the heat flux from the water to air, the greater the convective driver and the deeper the plume will develop into the CITBL.

Presently there are no systems available to observe this phenomenon other than by the use of nephelometers and transmissonmeters. These measurement devices are suited for scientific studies of specific areas, but are not practical for operational deployment in a potentially hostile coastal target area. The best tool for forecasting electro-optical system performance across the surf zone is by employing knowledge of the beach slope/breaker type characteristics, observing the temperature differences between the land and sea areas, and most importantly employing the understanding of the generation of surf aerosols coupled with the local mesoscale wind field and its effect on the modification of the aerosol plume structures.

A better understanding of the turbulence scales and surf aerosol production mechanisms are needed. Knowledge of the processes involved in the generation of these surf aerosols is imperative for determining their impact on EO systems. This research needs to be coupled with actual strike exercises on coastal targets to assess the operational impact on the IR/EO weapons systems currently employed and under development for coastal operations.

LIST OF REFERENCES

Bortkovskii, R. S., 1987: Air-sea exchange of heat and moisture during storms, Kluwer Academic Publishers, Norwell, MA, 194 pp.

Carlson, R., D. B. Law, C. Csanadi, G. Edwards and R. Tong, 1995: Thermal infrared transmission through the marine atmosphere boundary layer and LOWTRAN 7 predictions, NCCOSC RDTE DIV, San Diego, CA, Experiment Report (non-published), 10 pp.

Deirmendjian, D., 1969: Electromagnetic scattering on spherical polydispersions, American Elsevier, NY, 290 pp.

Fairall, C. W. and K. L. Davidson, 1986: Dynamics and modeling of aerosols in the marine atmospheric boundary layer, in:Oceanic Whitecaps, E. C. Monahan and G. MacNiocaill eds., D. Reidel Publishing Company, Dordrecht, NL, pp. 195-208.

Jensen, D. R., 1995: EO propagation assesment in the coastal environments, NCCOSC RDTE DIV Code 543, San Diego, CA, Collection of EOPACE Workshop Reports, May 1995, 80 pp.

Philbrick, R. C., F. Balsiger, T. Stevens, S. Mathur and W. Durbin, 1996: EOPACE surf aerosol data summary for phase I at Scripps Pier, Pennsylvania State University, (non-published), 36 pp.

Philbrick, R. C., S. Mathur, W. Durbin and R. Kiser, 1996: EOPACE data summary at Moss Landing, Pennsylvania State University, (non-published), 33 pp.

Pond, S., and G. L. Pickard, 1991: Introductory dynamic oceanography, Pergamon Press Inc., Elmsford, NY, 329 pp.

Resch, F., 1986: Oceanic air bubbles as generators of marine aerosols, in:Oceanic Whitecaps, E. C. Monahan and G. MacNiocaill eds., D. Reidel Publishing Company, Dordrecht, NL, pp. 101-112.

Stull, R. B., 1988: An introduction to boundary layer meteorology, Kluwer Academic Publishers, Norwell, MA, 666 pp.

INITIAL DISTRIBUTION LIST

		No. Copies
1.	**Defense Technical Information Center** **Cameron Station** **Alexandria, Virginia 22304-6145**	**2**
2.	**Library, Code 52** **Naval Postgraduate School** **Monterey, California 93943-5101**	**2**
3.	Commander Naval Meteorology and Oceanography Command Stennis Space Center, Mississippi 39529-5000	1
4.	Commander Space and Naval Warfare Systems Command (PMW-185) Washington D.C. 20363-5100 Attn: CAPT W. Shutt	1
5.	Commander Space and Naval Warfare Command (PMW-185-3B) METOC Systms Program Office Arlington, VA 22245-5200 Attn: CDR T. Sheridan	1
6.	Chief of Naval Research 800 North Quincy Street Arlington, Virginia 22217	1
7.	Applied Research Laboratory The Pennsylvania State University P.O. Box 30 State College, PA 16804-0030 Attn: Professor Philbrick	5
8.	Naval Research Laboratory, TOWS Stennis Space Center, Mississippi 39529-4004 Attn: Ken Ferer/E. Mozley	1

9. Oceanographer of the Navy — 1
Naval Observatory
34th and Massachusetts Avenue NW
Washington DC 20390-5000
Attn: Franceen George

10. Naval Research Laboratory — 1
Naval Postgraduate School Annex
Monterey, California 93940-5006
Attn: A. Goroch

11. Professor K. Davidson — 2
Meteorology Department, Code MR/DS
Naval Postgraduate School
Monterey, California 93943-5002

12. Professor C. Wash — 1
Meteorology Department, Code MR/WX
Naval Postgraduate School
Monterey, California 93943-5002

13. NCCOSC RDTE DIV 543 — 2
53170 Woodward Road
San Diego, California 92152-7385
Attn: Dr Jensen/R. Carlson

14. NCCOSC RDTE DIV 54 — 1
53570 Silvergate Avenue
San Diego, California 92152-5230
Attn: Dr J. H. Richter

15. Physics and Electronics Laboratory TNO — 1
Oude Waalsdorperweg 63
2509 JG The Hague
The Netherlands
Attn: Dr G. de Leeuw

16. Office of Naval Research — 1
Ballston Tower #1, Rm 428-2
800 N Quincy St
Arlington, Virginia 22217-5660
Attn: Dr S. Sandgathe, ONR 322AM